JOURNAL
OF
GEOMAGNETISM
AND
GEOELECTRICITY

VOL. XII NO. 2

SOCIETY
OF
TERRESTRIAL MAGNETISM AND ELECTRICITY
OF
JAPAN

1961
KYOTO

JOURNAL OF GEOMAGNETISM AND GEOELECTRICITY

EDITORIAL OFFICE: Society of Terrestrial Magnetism and Electricity of Japan, Geophysical Institute, Kyoto University, Kyoto, Japan

The fields of interest of this quarterly Journal are as follows:

Terrestrial Magnetism	Aurora and Night Airglow
Atmospheric Electricity	The Ozone Layer
The Ionosphere	Physical States of the Upper Atmosphere
Radio Wave Propagation	Solar Phenomena relating to the Above Subjects
Cosmic Rays	Electricity within the Earth

The text should be written in English, German or French. The price is set as 1 dollar per number.

The Editors

Motion of Low-Energy Solar Cosmic Ray Particles in the Earth's Magnetic Field

By Kunitomo SAKURAI

Geophysical Institute, Kyoto University

(Read October 31, 1960; Received December 10, 1960)

Abstract

We calculate the orbits of the low-energy solar cosmic ray particles in the earth's dipole magnetic field and then estimate on their asymptotic velocity vectors before entering this magnetic field. Although the incident region of these particles is restricted in the area of higher geomagnetic latitudes than 60°, it is clear that there are anisotropic effects, i.e. impact zone effects for the incidence of these particles. Furthermore, the precipitation lines of the incidence will be shown to be circular around the geomagnetic north pole.

Next, it will be shown from the comparison of the calculated results with the observed data that, in the initial stage of the incidence, these low-energy cosmic ray particles tend to impinge upon the earth anisotropically, in accordance with the expectation from the calculated results, and that, slightly before the onset of geomagnetic Sc storms, their anisotropic incidence changes into isotropic one, although there are some exceptional cases. Finally, criticisms and a possible explanation on the features of their incidence after the onset of geomagnetic Sc storms will be proposed.

1. Introduction

The observations and the detailed studies on the low-energy cosmic rays associated with solar flares are being carried on very actively at present (Anderson, 1958; Anderson, Arnoldy, Hoffman, Peterson and Winckler, 1959; Freier, Ney and Winckler, 1959; Hakura and Goh, 1959; Leinbach and Reid, 1959; Ney, Winckler and Freier, 1959; Thompson and Maxwell, 1960). In association with these investigations, the studies on the low energy end of the galactic cosmic rays have started, and now the knowledge of these cosmic rays is being accumulated (Simpson, 1960).

The investigations on these low-energy solar cosmic rays made clear in detail the relation of solar phenomena to the terrestrial magnetic disturbances, the acceleration mechanism of these particles, their propagation into interplanetary space and so on (Reid and Leinbach, 1959; Obayashi and Hakura, 1960; Winckler, 1960). The incidence of the low-energy solar cosmic ray particles to the earth was firstly made clear by Bailey (1957; 1959) from the study of the abnormal ionization of the ionosphere associated with the cosmic ray intensity unusual increase at February 23, 1956. Then during the I.G.Y., many high-altitude observations of these low-energy solar cosmic

rays were performed and some properties of these cosmic rays have been clarified.

In this paper, in section 2., we shall at first calculate in details the motion of these low-energy solar cosmic ray particles in the earth's dipole magnetic field and then show these results in some figures. Although a part of this calculation was already performed in a previous paper (Sakurai, 1960), we shall investigate here the orbits of these cosmic ray particles in more details. In section 3, we shall consider the mechanism of the incidence of these particles and feature of the variation of geomagnetic fields during the geomagnetic Sc storms.

2. Motion of the Solar Cosmic Ray Particles in the Earth's Dipole Magnetic Field

It seems that the low-energy solar cosmic ray particles, which are ejected from the sun associated with the flares and then accelerated in its outer atmosphere, will approach the earth while interacting with the plasma clouds or the electromagnetic fields supposed to be in the interplanetary space. We may suppose that, before these cosmic ray particles arrive near the earth, their orbits will deviate from the solar direction on account of the action of the interplanetary magnetic field because of their low energies (Gold, 1959; 1960; Hakura and Goh, 1959; Reid and Leinbach, 1959; Obayashi and Hakura, 1960; Sakurai, 1960). According to the studies by Hakura, Takenoshita and Otsuki (1958) and Obayashi and Hakura (1960), however, the incidence of these low-energy solar cosmic ray particles seems to show such characteristics as follows; when these particles impinge upon the polar latitude region of the earth before the onset of the geomagnetic Sc storms, there are some anisotropies for their incidence, which seem to show that the motion of these particles well agrees with the expectation from the theory of geomagnetic effect of cosmic rays (Sakurai, 1960). Since some time before the onset of the geomagnetic Sc storms, they will begin to impinge upon isotropically, and then come nearly uniformly into, the polar latitude region. This change of anisotropic into isotropic incidence appears to mean that, according to the present knowledge of the solar cosmic rays, the distribution of the low-energy solar cosmic ray particles in the interplanetary space becomes isotropic (Meyer, Parker and Simpson, 1956; Obayashi and Hakura, 1960). So, the incidence of these low-energy solar cosmic ray particles to the earth shows anisotropy at the initial stage and then gradually becomes isotropic, and before long they uniformly arrive at the polar latitude region. Hence, we can conclude that, in the initial stage of their incidence, these low-energy solar cosmic ray particles will arrive near the earth with some anisotropies. From such a point of view, we calculated in a previous paper (Sakurai, 1960) the paths of the low-energy cosmic ray particles approaching the earth in the solar direction. In this paper, we shall calculate the motion of these particles in more details and then examine their orbits in the earth's magnetic field and the features of their precipitation on the earth.

At first, as shown in Fig. 1, let the latitude of observing points be λ (degrees), and the asymptotic velocity vectors of the cosmic ray particles impinging vertically upon the earth be $(\lambda_\infty, \varphi_\infty)$, where λ_∞ and φ_∞ are latitude and longitude components

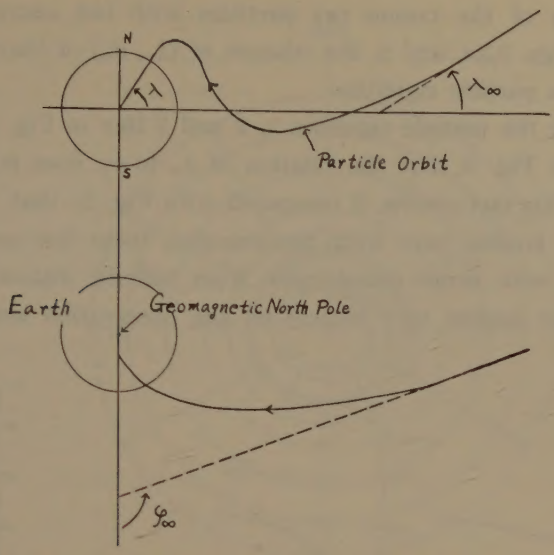

Fig. 1. Angle used to describe orbits of low energy cosmic rays coming from the sun and arriving vertically upon the earth, (from Firor (1954))
(a) Orbits in a meridian plane that moves with particle, showing the latitude of incidence, λ, the latitude of the asymptotic velocity vector, λ_∞;
(b) Projection of orbit on the equatorial plane. The angle φ_∞ is the longitude of impact relative to the source.

of these velocity vectors, respectively. As valuable works on these velocity vectors of the cosmic ray particles within Bev-rigidity range were already performed by many authors (Malmfors, 1945; Dwight, 1950; Schlüter, 1951; 1958; Firor, 1954; Brunberg, 1956; Jory, 1956; Lüst, 1957; 1958; Lüst and Simpson, 1957), we shall here

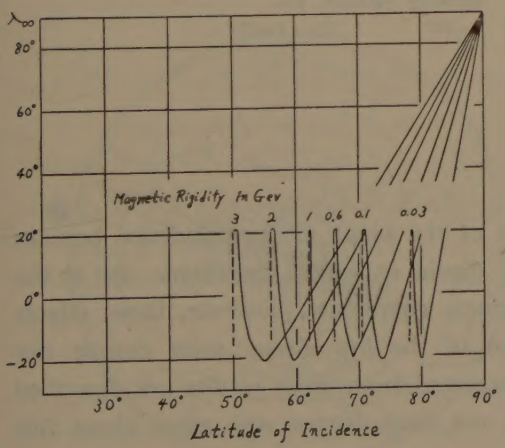

Fig. 2. Relation between the geomagnetic latitude of impact on the earth of particles arriving from the sun with magnetic rigidities of 30 Mev to 3 Bev, and the geomagnetic latitude of source (Sakurai, 1960).

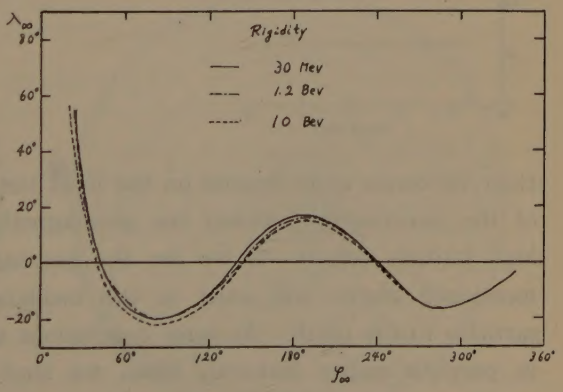

Fig. 3. Relation between the geomagnetic longitude of impact on the earth of particles arriving from the sun with magnetic rigidities of 30 Mev, 1.2 Bev, and 10 Bev, and the latitude of the source (Sakurai, 1960).

calculate the motion of the cosmic ray particles with low energies of Mev range. We shall show, in Figs. 2,3,4, and 5, the relation of $(\lambda_\infty, \varphi_\infty)$ of the cosmic ray particles arriving at λ to these particle rigidities.

The results about the particle rigidities 1, 2 and 3 Bev in Fig. 2 are due to Firor (1954). We see from Fig. 3 that the relation of λ_∞ to φ_∞ does not depend upon the particle rigidities. This fact shows, if compared with Fig. 2., that, in similar manners as the incidence of cosmic rays with Bev-energies, these low-energy particles also approach the earth with some anisotropies from infinite distance. These impact zone effects may not appear very clearly on the observation since the features of

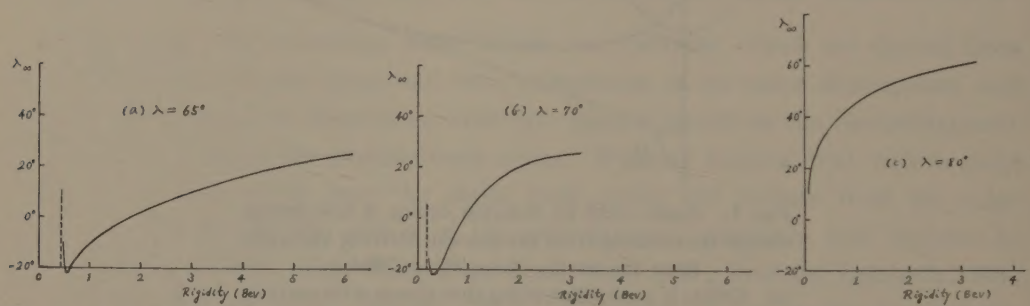

Fig. 4. Particle rigidities arriving at geomagnetic latitude λ and the latitude component of the asymptotic velocity vectors, λ_∞.
(a) $\lambda=65°$ (b) $\lambda=70°$ (c) $\lambda=80°$

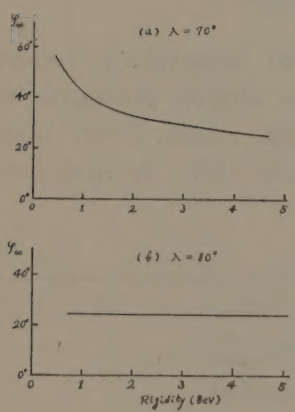

Fig. 5. Particle rigidities arriving at geomagnetic latitude λ and the longitude component of the asymptotic velocity vectors, φ_∞.
(a) $\lambda=70°$ (b) $\lambda=80°$

their incidence quite depend on the local time of the onset of the incidence because of the discrepancy between the geomagnetic dipole axis and geographic one in the high latitude region. If we use the geomagnetic coordinate, however, those effects mentioned above will exist in the incidence of the low-energy solar cosmic ray particles to the earth. As some conclusions expected from those results are described in previous paper (Sakurai, 1960), we shall not here discuss any more about this problem.

In the next place, we shall examine about the precipitation of the low-energy solar cosmic ray particles on the earth. We shall study the precipitation lines of their vertical incidence using the geomagnetic coordinates, and then show the results

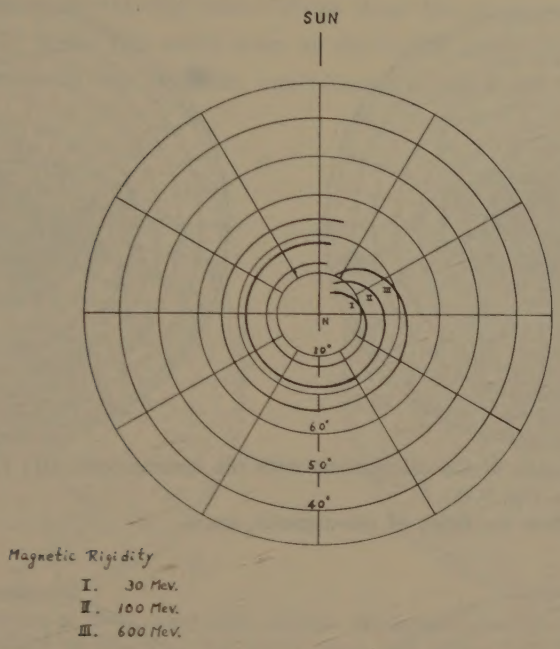

Fig. 6. Precipitation lines of low rigidity particles coming from the sun on the earth.
N: geomagnetic north pole.

in Fig. 6. The center of this coordinate is the geomagnetic north pole, and we take the solar direction upward. These forms are the same as those of Störmer (1955), who used them to explain the formation of the auroral zone. This figure shows in what manner the low-rigidity particles coming near the earth along the straight paths in the solar direction will impinge upon the earth. As evident from this figure, their

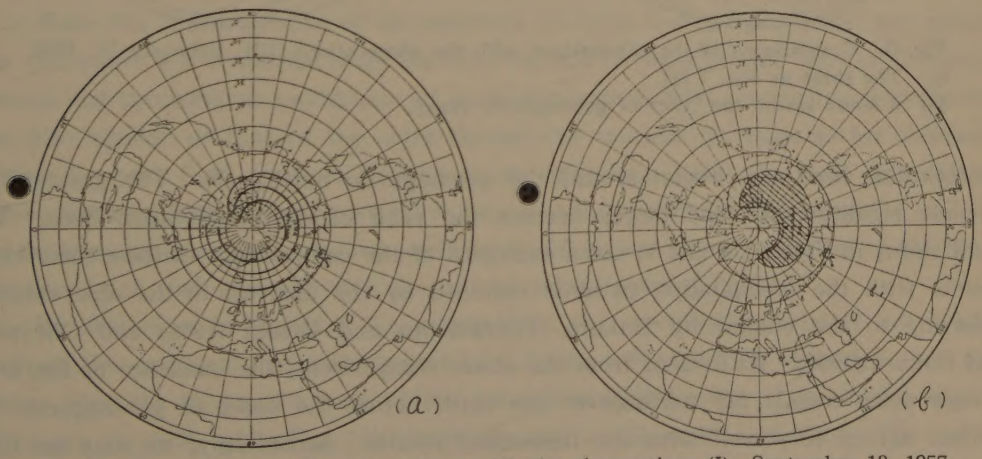

Fig. 7. Comparisons of the calculations with the observations (I); September 13, 1957.
⊙ shows solar direction.
(a) Precipitation lines of low-rigidity particles (30 Mev, 100 Mev and 600 Mev)
(b) The incidence of these particles before the onset of geomagnetic storm (7 hours before)

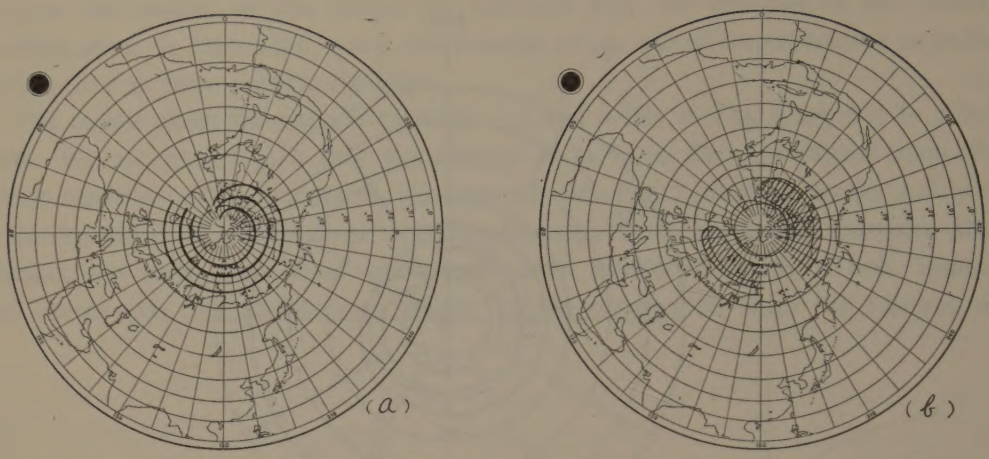

Fig. 8. Comparisons of the calculations with the observations (II); February 11, 1958.
(a) The same as Fig. 7 (a).
(b) 11 hours before the onset of geomagnetic storm.

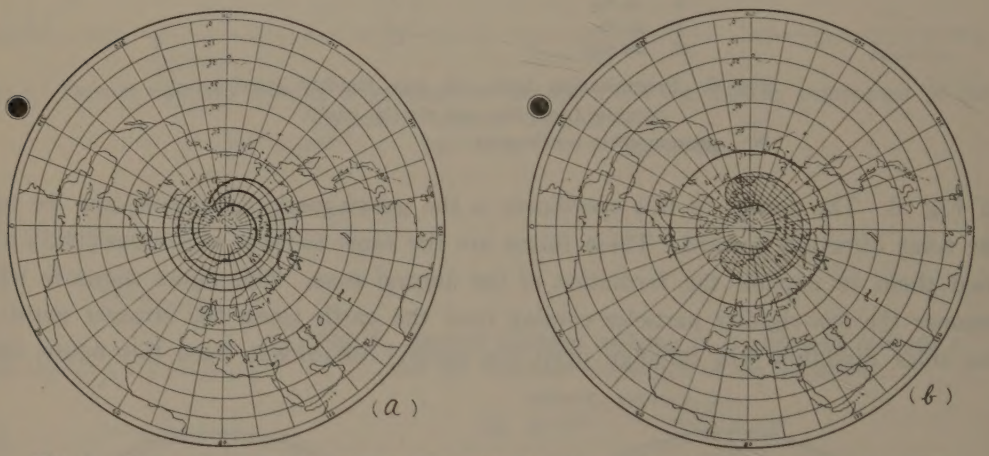

Fig. 9. Comparisons of the calculations with the observations (III); February 11, 1958.
(a) The same as Fig. 7 (a).
(b) 6 hours before the onset of geomagnetic storm.

precipitation lines are circular around the geomagnetic north pole. The greater the particle rigidities are, the larger become the radii of the precipitation lines. We shall show, in Figs. 7, 8 and 9, some examples of the comparisons of these theoretical results with the precipitation patterns obtained by the analyses of the observations, referring to the studies by Hakura, Takenoshita and Otsuki (1958) and Obayashi and Hakura (1960). As evident from the above comparisons, the incidence of the low-energy solar cosmic ray particles to the earth before the onset of geomagnetic Sc storms agrees very well with the theoretical results. Accordingly, we may see that the interplanetary space long before the onset of geomagnetic Sc storms is magnetically clean so as to be non-effective on the propagation of these particles.

There are, however, some instances which are against what has just been said.

Since there are some observational cases where these low-energy cosmic ray particles impinge isotropically upon the earth even at the initial stage of their incidence (Fig. 10), we cannot necessarily say that the interplanetary space are always magnetically

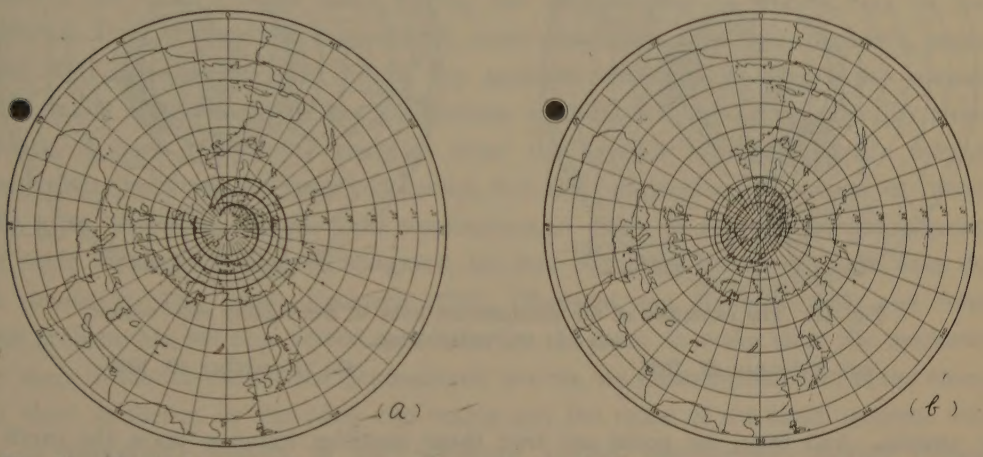

Fig. 10. The incidence of low-energy solar cosmic ray particles on Oct. 21, 1957. This figure shows the isotropic incidence at the initial stage, and differs from Figs. 7, 8 and 9.

clean. Consequently, such examples as shown in Figs. 7, 8 and 9 might be rather exceptional. Some recent studies on the low-energy solar cosmic ray events seem indeed to show that the incidence of these particles is isotropic from the initial stages (Reid and Leinbach, 1959; Leinbach, 1960), but, because the statistical analysis by Hakura (1960) on some low-energy solar cosmic ray events shows the clear existence of their anisotropic incidence before the onset of geomagnetic Sc storms, we may see that, statistically speaking, the low-energy solar cosmic ray particles will impinge upon the earth rather anisotropically at the initial stage of their incidence.

Since the characteristics of the incidence of these low-energy cosmic ray particles to the earth are consistent with the observations on solar cosmic rays of Bev-energy range, the propagation mechanism of these low-energy solar cosmic ray particles may be also similar to that of the solar cosmic ray unusual increases so far observed 6 times (Cocconi, Gold, Greisen, Hayakawa and Morrison, 1958; Obayashi and Hakura, 1960; Sakurai, 1960). Hence, we may infer that the impact zone effects of the incidence of the low energy solar cosmic ray particles do not appear sharply because of the strong interaction in their passage with the interplanetary magnetic fields.

We shall show in Fig. 11 a few examples of the precipitation lines of solar cosmic rays of Bev-energy range with respect to 1, 2 and 3 Bev particle rigidities at a fixed time. Fig. 11a shows the case of the solar cosmic ray event at the initial stage on February 23, 1956, while Fig. 11b shows the case on November 19, 1949. The hatched areas in these figures show the impact zones in both events mentioned above.

We have examined, in this section, the characteristics of the incidence of the low-energy solar cosmic ray particles to the earth before the onset of geomagnetic

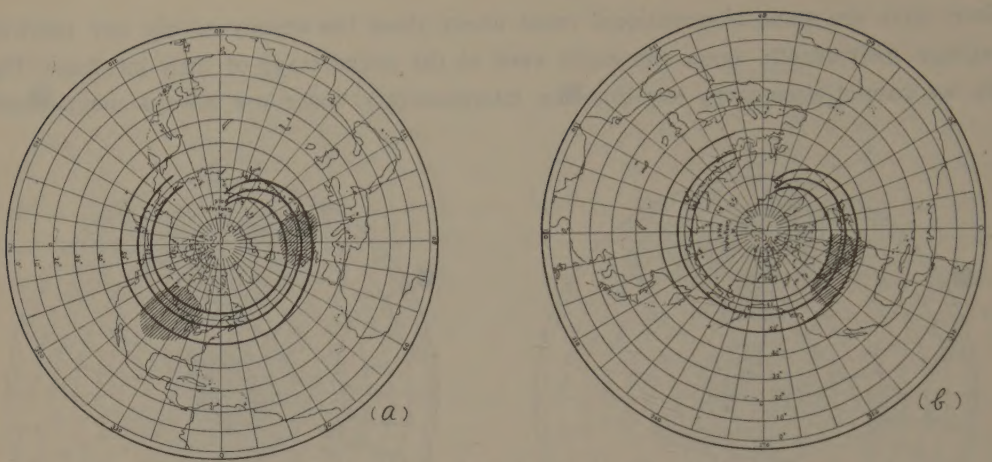

Fig. 11. The examples of the precipitation lines of Bev-rigidity solar cosmic rays at the initial stage.
(a) February 23, 1956 (b) November 19, 1949

Sc storms. And then, we could see that these particles impinge upon the earth in accordance with the expectation from the calculated results on their orbits (Figs. 7, 8 and 9). On the other hand, there are some cases in which their orbits are much disturbed by the influence of the interplanetary magnetic fields (Fig. 10). We can, therefore, conclude that the propagation mechanism of these low-energy solar cosmic ray particles may always be controlled by the physical states of the interplanetary space. In the next section, we shall consider the behavior of these low-energy solar cosmic ray particles after the onset of geomagnetic Sc storms.

3. Geomagnetic Storm Effects upon the Incidence of Low-Energy Solar Cosmic Ray Particles

According to the studies of Hakura, Takenoshita and Otsuki (1958) and Obayashi and Hakura (1960), the incident region of the low-energy solar cosmic ray particles, after the onset of geomagnetic Sc storms, extends southwards beyond the polar cap region and shows spiral structures. Since the southward shifting of this incident region is very remarkable, it seems that there is a mechanism, in the outer space around the earth, quite different from that of the incidence of these particles before the onset of geomagnetic Sc storms discussed in section 2.

We shall consider in this section the geomagnetic storm effects on such incidence of the low-energy solar cosmic ray particles. It is clear that the earth's dipole magnetic field extends fairly far (say, 13 earth radii) if the geomagnetic storm producing solar plasma does not surround the earth (Sonett, Judge and Kelso, 1959; Sonett, Judge, Sims and Kelso, 1960). Such an extension of the earth's dipole magnetic field was pointed out theoretically by Dungey (1955), and furthermore, the interplanetary plasma appears to confine the geomagnetic fields within the domain around the earth. It is, at present, inferred that, if the geomagnetic storm producing plasma surrounds

the earth, the earth's magnetic fields will be confined within the domain of several earth radii from the earth (Chapman and Ferraro, 1932; Parker, 1958c; Dessler and Parker, 1959).

In consequence, we can easily see that the distribution of the earth's magnetic field in the earth's outer space during the geomagnetic Sc storms may be quite different from that on the magnetically quiet conditions. We may, therefore, suppose that, if the low-energy solar cosmic ray particles interact with the earth's magnetic field in its disturbed state, the conclusions in section 2 will be considerably altered. Hence, if these cosmic ray particles enter the severely disturbed earth's magnetic field, their paths will be largely deflected, and their directions will become at random. We must, therefore, assume some mechanisms in order to explain the characteristics of their incidence during geomagnetic storms. Although such trials have been done in details by Ray (1956), Rothwell (1959), Obayashi and Hakura (1960) and others, this problem has not been solved satisfactorily. In order to make clear the mechanism of their incidence during the geomagnetic storms, we must explain both of the absence of their incidence in the polar cap region and the cause of the spiral pattern, which is a remarkable feature in the incidence during geomagnetic storms (Hakura, Takenoshita and Otsuki, 1958; Obayashi and Hakura, 1960). For the complete explanation of this feature, it is necessary to know the states of the earth's outer atmosphere in detail.

Recently, Dungey (1958) considered theoretically the distribution of the magnetic fields of stars within their outer atmosphere and showed that these magnetic fields were confined within the restricted domain around them by the interaction with interstellar plasmas. As shown by Ferraro (1937), Lüst and Schlüter (1955) and Cowling (1957), this result is also proved from the theoretical studies on the stellar magnetic fields. In view of these studies, we may infer that the forms in the outer space of the magnetic lines of force intersecting with the polar latitude region of the earth are quite different from those with low latitude regions (Hines, 1960). We may, therefore, suppose that very complicated phenomena will occur in the polar latitude region on geomagnetically disturbed conditions. And then, a configuration of the earth's magnetic field, which forbids the incidence during geomagnetic storms of the low-energy solar cosmic ray particles to the polar latitude region, will be formed in the earth's outer space. We do not yet know, at present, the theory by which the motion of the low-energy solar cosmic ray particles in the earth's magnetic field during geomagnetic storms can be explained fairly. A qualitative consideration on this problem is presented by Winckler and Bhavser (1960), but, as this cannot explain it in details, we must continue to study the mechanism of their incidence during geomagnetic storms.

In concluding, we must hereafter proceed to examine this unsolved problem since we can explain, as shown in section 2, the characteristics of their incidence before the onset of geomagnetic Sc storms.

4. Concluding Remarks

The low-energy cosmic ray particles produced at the sun will propagate into the interplanetary space and then, interacting with the earth's magnetic field, they will impinge upon the polar latitude region of the earth. We showed in section 2. that these cosmic ray particles impinge upon the earth at the initial stage of the incidence before the onset of geomagnetic Sc storm in accordance with the expectation from the theoretical results on their orbits (Figs. 7, 8 and 9). Hence, we can see that, when these particles propagate into the interplanetary space, they will approach the earth without the directions of their paths being much disturbed. Since we also know some cases where they have already impinged isotropically upon the earth even at the initial stage (Fig. 10), we cannot conclude that the interplanetary space is always transparent for their propagation. The propagation mechanism shown in a previous paper (Sakurai, 1960) will be able to explain the above observations.

In consequence, the investigations on the low-energy solar cosmic ray events will be powerful means to make clear the properties and variabilities of the physical states of the interplanetary space. In particular, as shown in section 3, we do not stand on the satisfactory ground for the explanation of the incidence of these cosmic ray particles during geomagnetic storms, so we must continue to investigate this problem in future. The solutions of the mechanism of geomagnetic Sc storms and states of the earth's outer atmosphere during these storms will settle this problem completely.

Acknowledgement

The author wishes to express his hearty thanks to Prof. Y. Tamura and Prof. M. Hasegawa for their kind advice and encouragement, and to Prof. K. Maeda and Dr. H. Maeda for their helpful discussions and criticisms on this work. He is also due to Mr. H. Leinbach, Dr. T. Obayashi and Dr. Y. Hakura for their valuable discussions and suggestions.

References

Anderson K.A. (1958) Phys. Rev. Lett. **1**, 335.

Anderson K.A., Arnoldy R., Hoffman R., Peterson L. and Winckler J.R. (1959) J. Geophys. Res. **64**, 1133.

Bailey D.K. (1957) J. Geophys. Res. **62**, 431.

Bailey D.K. (1959) Proc. IRE. **49**, 255.

Brunberg E. (1956) Tellus 8, 215.

Chapman S. and Ferraro V.C.A. (1932) Terre. Mag. **37**, 147.

Chapman S. and Ferraro V.C.A. (1932) Terre. Mag. **37**, 421.

Cocconi G., Gold T., Greisen K., Hayakawa S. and Morrison P. (1958) Nuovo Cim. Supp. 8, 161.

Cowling T.G. (1957) Magnetohydrodynamics; Interscience Publ.

Dessler D.J. and Parker E.N. (1959) J. Geophys. Res. **64**, 2239.

Dungey D.W. (1955) Rep. Phys. Soc. Conf. on Phys. of Ionosphere at Cavendish Lab. Cambridge,

Sep. 1954.
Dungey D.W. (1958) Cosmic Electrodynamics; Cambridge Univ. Press.
Dwight K. (1950) Phys. Rev. **78**, 40.
Ferraro V.C.A. (1937) M.N. **97**, 458.
Firor J. (1954) Phys. Rev. **94**, 1017.
Freier P.S., Ney E.P. and Winckler J.R. (1959) J. Geophys. Res. **64**, 685.
Gold T. (1959) J. Geophys. Res. **64**, 1665.
Gold T. (1960) Ap. J. Supp. **4**, 406.
Hakura Y., Takenoshita Y. and Otsuki T. (1958) Rep. Ionos. Res. Japan **12**, 459.
Hakura Y. and Goh T. (1959) J. Radio Res. Lab. **6**, 635.
Hakura Y. (1960) Lecture at the Society of Terre. Mag. and Electr. Japan, May 1960, Tokyo.
Hines C.O. (1960) J. Geophys. Res. **65**, 141.
Jory F.S. (1956) Phys. Rev. **103**, 1068.
Leinbach H. (1960) Private Communication.
Leinbach H. and Reid G.C. (1959) Phys. Rev. Lett. **2**, 61.
Lüst R. (1957) Phys. Rev. **105**, 1827.
Lüst R. (1958) Nuovo Cim. Supp. **8**, 176.
Lüst R. and Schlüter A. (1955) Z.f. Astrophys. **38**, 190.
Lüst R. and Simpson J.A. (1957) Phys. Rev. **108**, 1563.
Malmfors K.G. (1945) Ark. för Mat. Astr. Fys. **32A**, 1.
Meyer P., Parker E.N. and Simpson J.A. (1956) Phys. Rev. **104**, 768.
Ney E.P., Winckler J.R. and Freier P.S. (1959) Phys. Rev. Lett. **3**, 183.
Obayashi T. and Hakura Y. (1960) J. Radio Res. Lab. **7**, 27.
Parker E.N. (1958a) Ap. J. **128**, 664.
Parker E.N. (1958b) The Plasma in a Magnetic Field, p. 77, ed. by Landshoff R.K.M.; Stanford Univ. Press.
Parker E.N. (1958c) J. Phys. Fluids **1**, 171.
Ray E.C. (1956) Phys. Rev. **101**, 1142.
Reid G.C. and Leinbach H. (1959) J. Geophys. Res. **64**, 1801.
Rothwell P. (1959) J. Geophys. Res. **64**, 2026.
Sakurai K. (1960) J. Geomag. Geoel. **11**, 152.
Schlüter A. (1951) Z.f. Naturforsch. **6a**, 613.
Schlüter A. (1958) Nuovo Cim. Supp. **8**, 349.
Simpson J.A. (1960) Ap. J. Supp. **4**, 378.
Sonett C.P., Judge D.L. and Kelso J.M. (1959) J. Geophys. Res. **64**, 941.
Sonett C.P., Judge D.L., Sims A.R. and Kelso J.M. (1960) J. Geophys. Res. **65**, 55.
Störmer C. (1955) Polar Aurora; Oxford Univ. Press.
Thompson A.R. and Maxwell A. (1960) Planet. Space Sci. **2**, 104.
Winckler J.R. (1960) J. Geophys. Res. **65**, 1331.
Winckler J.R. and Bhavser P.D. (1960) J. Geophys. Res. **65**, 2637.

On the Relativistic Electrons in the Solar Atmosphere

By Kunitomo SAKURAI

Geophysical Institute, Kyoto University

(Read October 31, 1960; Received December 10, 1960)

Abstract

We consider the various processes, in solar atmosphere, of the relativistic electrons ejected in association with flares and examine how these electrons will lose their energies.

In view of the above examination, we can show that these electrons will be trapped in the sunspot magnetic fields (~100 gauss) and then lose the majority of their energies through the synchrotron radiation. So, the radio waves emitted by these synchrotron radiation processes will be observed as the type IV outbursts.

1. Introduction

The behavior of the electron component associated with the acceleration of solar cosmic rays does not yet seem to have been made clear in details.

Recently, however, some theoretical studies on the emission mechanism of the solar radio type IV outbursts have supplied some new informations of the motion of high energy electrons in solar atmosphere (Boischot, 1957, 1959; Boischot and Denisse, 1957). At present, low-energy solar cosmic rays with energies ranging from some 10 Mev to several 100 Mev are being investigated, and the relation of these cosmic rays to the solar and terrestrial disturbances, or the propagation mechanism of these cosmic rays into interplanetary space and so on, have been made clear both experimentally and theoretically (Reid and Leinbach, 1959; Obayashi and Hakura, 1960; Winckler, 1960).

In this paper, we shall at first examine various processes, in solar atmosphere, of the electrons ejected in association with flares. And then, we shall consider the behavior of the relativistic electrons in solar atmosphere. Next, we shall present a possible explanation of the solar radio type IV outbursts.

2. Relativistic Electrons in Solar Atmosphere

The production of low-energy cosmic rays from the sun associated with flares was recently made clear by many authors (Bailey, 1957, 1959; Reid and Leinbach, 1959; Simpson, 1960; Winckler, 1960). Furthermore, the production of low-energy solar cosmic rays is closely associated with the emission of the solar radio type IV outbursts (Boischot and Denisse, 1957; Hakura and Goh, 1959).

These facts suggest that the existence of the protons with energies ranging from

a few Mev to several 100 Mev in solar atmosphere will show that of the electrons with energies of the same orders. It will, therefore, be necessary to examine how the electron component will behave during the acceleration of solar cosmic rays.

Both of protons and electrons ejected with solar flares will be accelerated or decelerated through their interaction with plasma and electromagnetic fields in solar atmosphere. Since the rates of energy loss of these protons through the interaction with solar plasma are negligibly small as shown by Hayakawa and Kitao (1956) and Parker (1957), it is clear that the acceleration of the proton component in solar atmosphere is possible enough. Then, for an acceleration mechanism, the Fermi

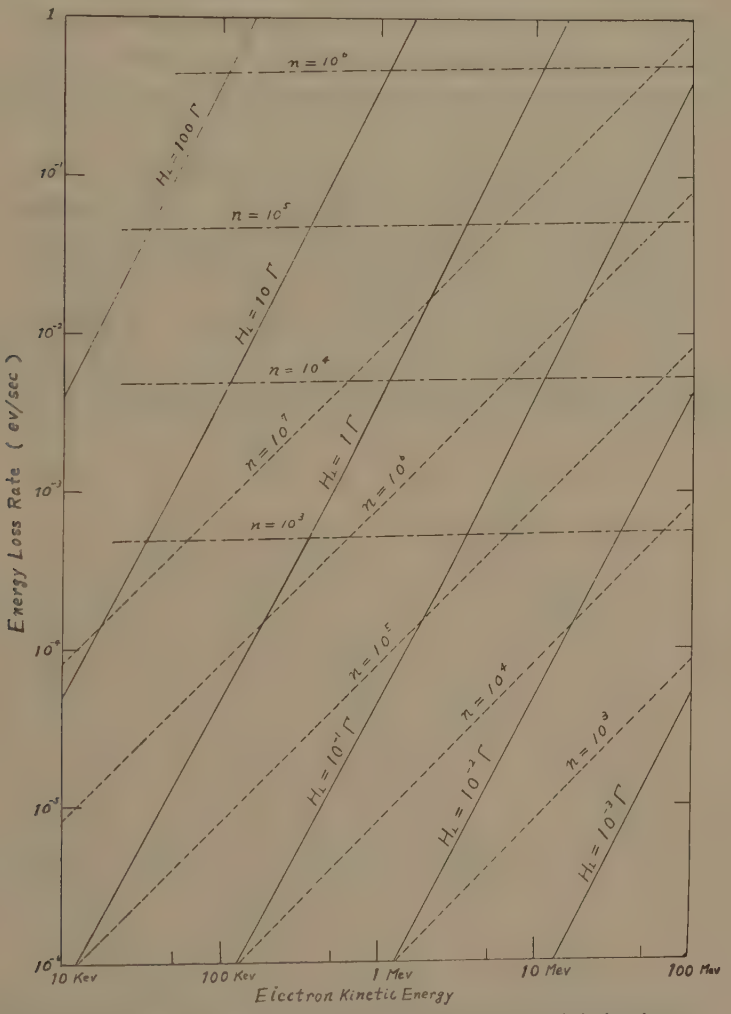

Fig. 1. Various processes of energy loss of the relativistic electron. The energy loss rates are shown with respect to electron kinetic energy.

———: synchrotron radiation loss.

— — — —: ionization loss.

– – – – – –: radiation loss.

n, $H_\perp$ show the electron number density per cm³ and magnetic field intensity (gauss) in a medium.

mechanism is proved to be most effective (Fermi, 1949; Parker, 1957, 1958a). Hence, the proton component will be well accelerated to cosmic ray energies. Furthermore, the studies on the suprathermal particles have recently made a progress, and their results are applied to explain the acceleration of low-energy solar cosmic rays and the observed characteristics of these particles (Parker, 1958b; Parker and Tidman, 1958; Obayashi and Hakura, 1960). On the contrary, it is clear from Fig. 1 that the electron component will be decelerated rather than accelerated because its ionization energy loss rate is very large in solar atmosphere. Our following discussion, therefore, will be limited on the deceleration of these electrons.

The electrons ejected into solar atmosphere in association with a flare will undergo various interactions with magnetic clouds there. Because the rate of electron acceleration is negligible, we shall examine various deceleration processes such as ionization energy loss, radiation effect and synchrotron radiation, and estimate these energy loss rates using electron number densities and magnetic field intensities as parameters. In order to estimate these rates, we here use the formulae derived by Heitler (1954), Ginzburg (1958) and Hayakawa, Ito and Terashima (1958). These estimations are shown in Fig. 1. From this figure we can see that, if the electron energies are in Mev-range, the energy loss rate by synchrotron radiation is most important in the strong magnetic field in outer atmosphere. In other words, as the electron densities in solar outer atmosphere (~a few solar radii) are very small, the energy loss rates by ionization and radiation become negligibly small and, in the strong magnetic fields (≧100 gauss),

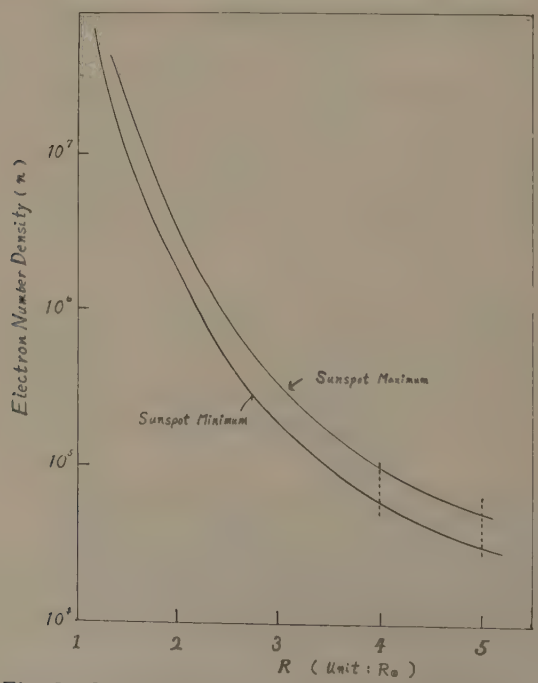

Fig. 2. The distribution of the electron number density in the solar outer atmosphere.
$R_\odot$ shows the radius of the sun ($=7\times10^{10}$cm).

the synchrotron radiation loss process is more important than the above two processes. In the solar inner atmosphere, however, the ionization process is very effective as seen from Figs. 1 and 2. The data shown in Fig. 2 are due to Allen (1955). The radiation process is negligible in the outer atmosphere. In case of the magnetic field intensities are $\lesssim$10 gauss, the ionization process is most important and, if the intensity is greater than 100 gauss, the synchrotron radiation process becomes most effective. We note here that the electron kinetic energy range in the above discussion is from 10 Kev to 1000 Kev (=1 Mev).

From the previous discussion, we may infer that, after ejected into solar atmosphere, the proton component will be accelerated to cosmic ray energies and propagate into interplanetary space and that the electron component will be decelerated mainly through the ionization process in the weak magnetic field regions or through the synchrotron radiation process in such strong magnetic field regions as sunspots ($\gtrsim$100 gauss).

Since it has been guessed that the solar radio type IV outbursts are due to the synchrotron radiation of relativistic electrons (Boischot, 1957, 1959), we can see that the type IV outbursts are made by the electromagnetic radiation emitted through the interaction of the relativistic electrons with the sunspot magnetic fields because of the close association of the solar flares with the sunspot magnetic field configuration (McLean, 1959; Takakura, 1959). Pretty high correlation of the solar radio type IV outbursts with the low-energy solar cosmic ray events may show that both of protons and electrons will undergo the processes mentioned above (Hakura and Goh, 1959; Obayashi and Hakura, 1960; Sakurai, 1960; Thompson and Maxwell, 1960).

3. A Possible Explanation of Type IV Outbursts

As shown in the last section, the relativistic electrons ejected into solar atmosphere, associated with flares, will lose the majority of their energies within the domain of several solar radii from the sun while emitting the electromagnetic radiation. Thus, these relativistic electrons will disappear in solar atmosphere, so they will not propagate into interplanetary space. The large dispersion of the emitting sources of type IV outbursts, ranging from 1.2 to about 5 solar radii, leads us to conclude that the emitting sources will move actively in solar atmosphere. And then, as the number of relativistic electrons ejected from the sun will be extremely large in the low energy end, considerably strong magnetic field of the order of 100 gauss must exist in the solar outer atmosphere in order to explain the observations of the type IV outbursts. A possible explanation, therefore, is as follows: After the high energy protons and electrons are ejected into solar atmosphere in association with flares, they will transport upward the surrounding sunspot magnetic fields. Thus, we may suppose that, even within the solar outer atmosphere, the strong magnetic field of several 100 gauss exists at the time of these disturbances. These electrons will consequently lose their energies through the synchrotron radiation which is caused by their interaction with the sunspot magnetic fields stretched out by the solar plasma. So, we may observe

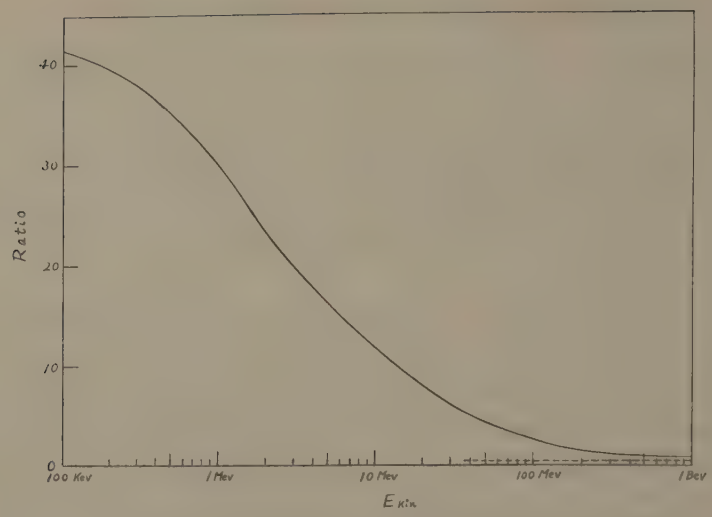

Fig. 3. The ratio of the proton magnetic rigidity to the electron's shown with respect to the kinetic energy (see Appendix 1).

these processes as solar radio type IV outburst.

In Fig. 3, we shall show the ratio of the proton magnetic rigidity to that of electron in regard to the same kinetic energy (Appendix 1.). Since this ratio is very large as seen from this figure, it seems that the trapping of these electrons in magnetic fields is much easier than that of the proton. Hence, we may interpret that, while the proton component will escape more easily from the magnetic fields extended into the solar outer atmosphere, the electron component will be unable to do so and they will lose there the majority of their energies.

The duration, so-called half-life, of the emissions of the type IV outbursts is ranging from about 20 minutes to 1.5 hours. Taking into account these values, we shall show in Fig. 4 the relation of the electron initial kinetic energies to the magnetic field intensities $H_\perp$ (gauss unit), where $H_\perp$ is a component of magnetic field (H) perpendicular to the electron velocity vector. We can also see from this figure that the relativistic electrons will lose their energies mainly through the synchrotron radiation process.

In concluding, we can see that the cause of the type IV outbursts is due to the interactions of the relativistic electrons of energies of some ten to several hundred Kevs, associated with solar flares, with the sunspot magnetic fields extended into the outer atmosphere.

4. Conclusion

After ejected into solar atmosphere in association with solar flares, component of both protons and electrons will diffuse into the outer space, undergoing various processes. The proton components will propagate into interplanetary space after accelerated to cosmic ray energies. On the other hand, since the deceleration processes are very important for the electron components, they will lose their energies through the

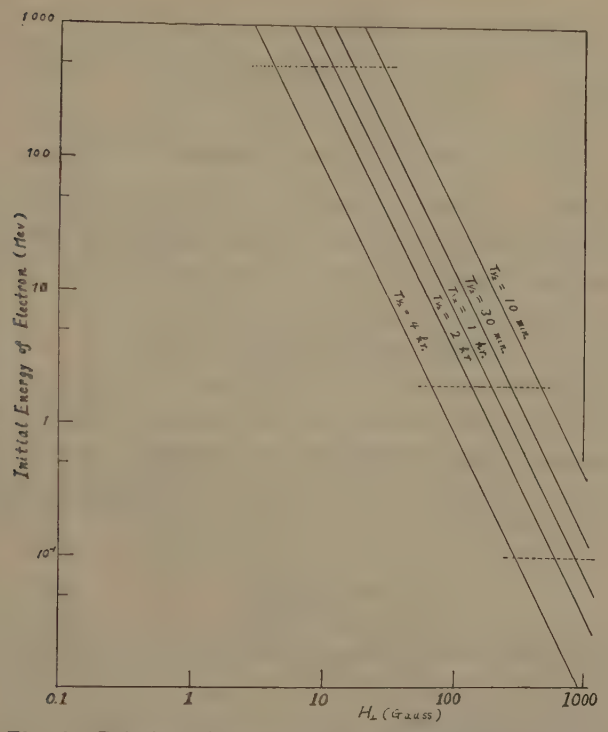

Fig. 4. Relation of the magnetic field intensity ($H_\perp$) with the electron initial kinetic energy, where the half-life of synchrotron radiation ($T_{1/2}$) are used as parameters.

ionization and the synchrotron radiation.

We can interpret the observations of the type IV outbursts on the basis of the assumption that there are strong magnetic fields of the order of 100 gauss in the solar outer atmosphere, which are extended by solar plasmas; in other words, these outbursts will be produced by the interaction of electrons with the sunspot magnetic fields.

Acknowledgement

The author wishes to express his sincere thanks to Prof. M. Hasegawa and Prof. Y. Tamura for their kind advice and encouragement. His thanks are also due to Prof. K. Maeda and Dr. H. Maeda for their valuable discussions and criticisms throughout the study.

Appendix 1.

Ratios of the Proton-to the Electron Magnetic Rigidity

Kinetic energy, momentum and magnetic rigidity of a charged particle (charge Ze; rest mass m) are expressed as follows:

$$\text{kinetic energy} \quad E_{kin}=mc^2\left[\frac{1}{\sqrt{1-\beta^2}}-1\right], \qquad (1)$$

$$\text{momentum} \quad P=\frac{mc\beta}{\sqrt{1-\beta^2}}, \tag{2}$$

$$\text{and magnetic rigidity} \quad \frac{Pc}{Ze}=\left\{\frac{E_{kin}(E_{kin}+2mc^2)}{(Ze)^2}\right\}^{1/2}, \tag{3}$$

where c is light velocity and $\beta=\frac{v}{c}$, v being a particle velocity.

We shall use here a suffix "p" and "e" for proton and electron respectively. The ratio of the proton rigidity to that of electron can be shown in the following form, if kinetic energies of both particles are quivalent ($Z=1$).

$$\frac{\text{Proton magnetic rigidity}}{\text{Electron magnetic rigidity}}=\left\{\frac{E_{kin}+2m_pc^2}{E_{kin}+2m_ec^2}\right\}^{1/2}, \tag{4}$$

where $E_{kin,p}=E_{kin,e}=E_{kin}$.

The results deduced from equation (4) are shown in Fig. 3. We can see that, as the electron rigidity is much smaller than the proton's even if the electron kinetic energy is the same as the proton's, the electrons will be easily trapped in the magnetic fields.

References

Allen C.W. (1955) Astrophysical Quantities; De Graff.

Bailey D.K. (1957) J. Geophys. Res. **62**, 431.

Bailey D.K. (1959) Proc. IRE. **49**, 255.

Boischot M.A. (1957) Compt. Rend. **244**, 1326.

Boischot M.A. (1959) Paris Symposium on Radio Astronomy, p. 186. ed. by Bracewell R.N.; Stanford Univ. Press.

Boischot M.A. and Denisse J.F. (1957) Compt. Rend. **245**, 1294.

Fermi E. (1949) Phys. Rev. **75**, 1169.

Ginzburg V.L. (1958) Prog. Elementary Particles and Cosmic Ray Physics Vol. IV, p. 339; ed. by Wilson J.G. et al., North-Holland Publ.

Hayakawa S. and Kitao K. (1956) Prog. Theor. Phys. **16**, 139.

Hayakawa S., Ito K. and Terashima Y. (1958) Prog. Theor. Phys. Supp. No. 6.

Hakura Y. and Goh T. (1959) J. Radio Res. Lab. **6**, 635.

Heitler W. (1954) Quantum Theory of Radiation 3rd ed.; Oxford Univ. Press.

McLean D.J. (1959) Austr. J. Phys. **12**, 404.

Obayashi T. and Hakura Y. (1960) J. Radio Res. Lab. **7**, 27.

Parker E.N. (1957) Phys. Rev. **107**, 830.

Parker E.N. (1958a) Phys. Rev. **109**, 1328.

Parker E.N. (1958b) Ap. J. **128**, 677.

Parker E.N. and Tidman D.A. (1958) Phys. Rev. **111**, 1206.

Reid G.C. and Leinbach H. (1959) J. Geophys. Res. **64**, 1801.

Sakurai K. (1960) J. Geomag. Geoele. **11**, 152.

Simpson J.A. (1960) Ap. J. Supp. **4**, 378.

Takakura T. (1959) Paris Symposium on Radio Astronomy, p. 562, ed. by Bracewell R.N.; Stanford Univ. Press.

Thompson A.R. and Maxwell A. (1960) Planet. Space Sci. **2**, 104.

Winckler J.R. (1960) J. Geophys. Res. **65**, 1331.

On the Origin of V.L.F. Noise in the Earth's Exosphere

By Tadanori ONDOH

Geophysical Institute, Kyoto University

(Read November 1. 1960; Received December 16, 1960)

Abstract

At present, there are some theories being able to explain the frequency characteristic of dawn chorus. In these theories, the natural thermal noise excited in a manner similar to the operation of a travelling-wave tube, the Doppler shifted proton cyclotron radiation and the Cerenkov radiation are considered as the origin of V.L.F. noise in the earth's exosphere respectively. This paper indicates that the Cerenkov radiation will be the most effective with respect to the emission energy in the above mentioned mechanisms in the earth's exosphere and that Cerenkov radio emissions generated by high speed protons (1.4×10^4 km/sec) precipitating into the ionized exosphere along the earth's magnetic field may be excited simultaneously by the operation of the mechanism similar to a travelling-wave tube due to charged particles different from those causing the Cerenkov radiation relatively near the earth less than about 4 earth radii from the center of the earth and then propagate toward the earth in the whistler mode.

1 Introduction

Storey (1953) has pointed out that the audio-frequency phenomenon called "dawn chorus" is the sound of a distant origin and that its occurrence correlates strongly with geomagnetic activity.

Such a same result has been also reported by Allcock (1957).

Then, latitude effect on the diurnal maximum of dawn chorus activity has been found by Allcock (1957) and Pope (1957, 1960) as represented in Fig. 1. Allcock has made the hypothesis that dawn chorus signals are generated in the vicinity of the geomagnetic equatorial plane.

He has replotted the data of Fig. 1 as a polar graph of local geomagnetic time against the height above the equator of the geomagnetic line of force passing through the station and has shown that the curve fitting the data is characteristic of the locus of a positively charged incoming particle in the equatorial plane, and being deflected by the earth's magnetic field. Thus, from above mentioned facts we can certainly deduce that dawn chorus may be generated directly or indirectly by streams and bunches of high speed charged particles precipitating into the ionized exosphere in the presence of the earth's magnetic field. Next we review briefly some theoretical works concerning the emission mechanism of V.L.F. noise in the exosphere.

Gallet and Helliwell (1956, 1959) have proposed that V.L.F. noise emissions are

due to the selective amplification of low-level electromagnetic waves, such as caused by the natural thermal noise in the exosphere. This amplification mechanism is similar to the operation of a travelling-wave tube and the condition for the operation of this mechanism is completely satisfied relatively near the earth, less than about 4 earth radii.

Recently Barrington (1959) has suggested that the condition for coupling between the whistler mode and the space charge modes of the beam resulting in an amplification of the whistler mode seems likely for certain region of the exosphere, especially above 2000 km over the ground.

Thus it is appropriate that we seek the region, where the interaction between the whistler mode and the beam modes takes place, relatively near the earth above the ionosphere. MacArthur (1959) has suggested that dawn chorus may be due to Doppler-shifted radiation from protons which are rotating about the geomagnetic lines of force with the cyclotron frequency, but he has argued it concerning the frequency characteristic only. Veksler (1957) has suggested that the Cerenkov radio emissions are generated by charged particles moving along magnetic lines of force in plasma. It has been recently indicated by Ellis (1959) that V.L.F. phenomena are due to the Cerenkov radiation by high speed charged particles moving along the geomagnetic lines of force.

Here we discuss the effectiveness of above mentioned emission mechanism in the earth's exosphere from the point of view of emission energy and compare the emission energy of a possible more effective mechanism with observed values of V.L.F. noise at ground.

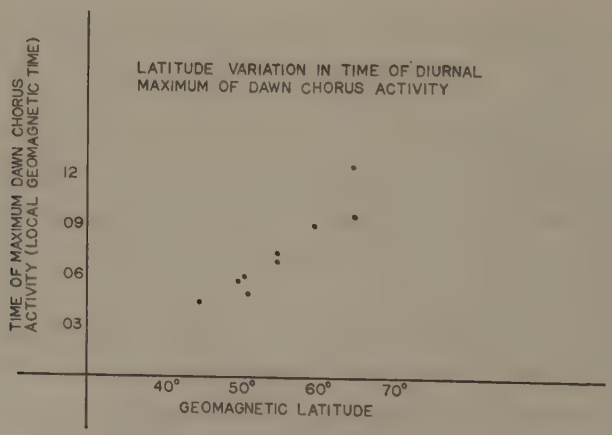

Fig. 1. Latitude Variation in Time of Diurnal Maximum of Dawn Chorus Activity (after Allcock)

2 The Origin of Dawn Chorus Deduced from Observed Facts

Allcock (1957) has found a marked variation of the time of maximum activity of dawn chorus with geomagnetic latitude from many data as shown in Fig. 1. Now we make the hypothesis that dawn chorus signals are generated relatively near the

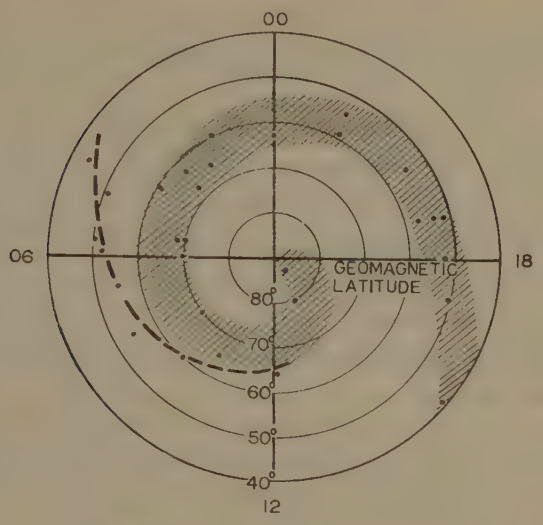

Fig. 2.

earth above the ionosphere by charged particles penetrating into the earth's exosphere. It is then appropriate to replot the data of Fig. 1 as a polar graph of local geomagnetic time of the diurnal maximum of dawn chorus activity against the geomagnetic latitude of each station. This is done in Fig. 2 with open points and a dotted curve. We can see that a dotted curve in Fig. 2 represents a spiral expanding in a clockwise.

On the other hand, Meek (1955) has used values of hourly averages for the year of "disturbed days minus quiet days" which Vestine (1947) has tabulated and charted from the 1932–33 Polar-Year data, and has made a polar plot of the local geomagnetic time of the diurnal maximum decrease in geomagnetic horizontal component for all available magnetic stations north of 40°N. This is represented by solid points and a shaded band that is also a spiral expanding in a clockwise in Fig. 2. These spirals expanding in a clockwise are characteristic of the Störmer's precipitation spiral of positively charged particles and we can see that the spiral concerning dawn chorus shifts toward lower latitudes than the spiral concerning geomagnetic horizontal component.

It is well known that geomagnetic disturbances at high latitudes are caused by charged particles impinging upon the ionosphere and the auroral zone gradually shifts southward as the corresponding storm grows intense (Nagata, 1949). From above facts, we can deduce that dawn chorus signals are generated by considerable high energy positively charged particles in the solar corpuscular stream.

3 A Possible More Effective Emission Mechanism of V.L.F. Noise in the Earth's Exosphere

Now we discuss which the proton cyclotron radiation or the Cerenkov radiation

due to protons is more effective with respect to the emission energy in the exosphere. We consider the longitudinal extraordinary propagation of V.L.F. noise in both cases in the exosphere.

The emission energy of the Cerenkov radiation and the proton cyclotron radiation at the frequency of 5 kc/s are estimated as 1.7×10^{-24} watts. m^{-3} and 7.2×10^{-28} watts. m^{-3} respectively at 2 earth radii from the center of the earth on the geomagnetic line of force passing through the earth's surface at the geomagnetic latitude of 60°. About this point in the exosphere, the electron density is $5\times10^3/cm^3$, which is deduced from the extrapolation of whistler observation (Ondoh and Hashizume, 1960), the velocity of protons is 10^9cm/sec, and the density of corresponding protons is $10^{-1}/cm^3$ which is of the order of auroral protons.

Thus the emission energy of the Cerenkov radiation is much greater than that of the proton cyclotron radiation under the same conditions in the exosphere. Hereafter we shall consider only the Cerenkov radiation as the origin of V.L.F. noise in the exosphere.

Then we review briefly the amplification mechanism similar to the operation of a travelling-wave tube given by Helliwell and Gallet (1956). By analogy with the small signal theory of travelling-wave tubes the necessary condition for coupling between the electromagnetic wave and the stream of charged particles is assumed to be $V=v_P$ where V is the velocity of the stream of ionized particles and v_P phase velocity of the electromagnetic wave.

For small propagation angle the quasi-longitudinal approximation holds good. In the whistler mode the local refractive index is $n=\left[1+\frac{f_0^2}{f(f_H-f)}\right]^{1/2}$ and $v_P=\frac{c}{n}$ where f is the wave frequency, f_0 the plasma frequency and f_H the electron gyro-frequency.

Combining v_P and n, we obtain the solutions of f which are given by

$$f=\frac{f_H}{2}\left[1\pm\left\{1-\left(2\frac{f_0}{f_H}\cdot\frac{V}{c}\cdot\frac{1}{\sqrt{1-\frac{V^2}{c^2}}}\right)^2\right\}^{1/2}\right].$$

For interaction to occur, f must be real and hence the condition for interaction to occur is $\left(2\frac{f_0}{f_H}\cdot\frac{V}{c}\right)^2\leqq 1$. The physical conditions of the exosphere for $\left(2\frac{f_0V}{f_Hc}\right)^2\ll 1$ will be satisfied relatively near the earth less than about 4 earth radii from the center of the earth.

Here we note especially the condition for interaction to occur and the frequency characteristic. As Ellis (1959) has suggested, the Cerenkov radio emissions due to charged particles moving along the geomagnetic line of force give the same type frequency characteristic as that of the mechanism given by Gallet and Helliwell. The condition for the Cerenkov radio emissions to occur is given by $V\cos\theta=\frac{c}{n}$ where V is the velocity of charged particles moving along the geomagnetic line of force and θ the angle between the wave normal direction and the geomagnetic line of force, c the velocity of light, and n the local refractive index for the extraordinary mode.

Combining $V\cos\theta=\frac{c}{n}$ and $n=\left[1+\frac{f_0^2}{f(f_H\cos\theta-f)}\right]^{1/2}$, we obtain the frequency of the Cerenkov radio emission of the extraordinary mode due to high speed charged particles moving along the geomagnetic line of force as

$$f=\frac{1}{2}f_H\cos\theta\left[1\pm\left\{1-\left(2\frac{f_0}{f_H}\cdot\frac{V}{c}\cdot\frac{1}{\sqrt{1-\frac{V^2}{c^2}\cos^2\theta}}\right)^2\right\}^{1/2}\right]$$

where f_0 is the plasma frequency, and f_H the electron gyrofrequency.

Generally the value of the expression $\frac{1}{\sqrt{1-\frac{V^2}{c^2}\cos^2\theta}}$ will be approximately equal to unity. For the Cerenkov radio emissions of the extraordinary mode to occur, f must be real and therefore the condition for the generation of Cerenkov radio emissions is $\left(2\frac{f_0}{f_H}\frac{V}{c}\right)^2\leqq 1$.

As shown by Gallet, at distances less than about 4 earth radii from the center of the earth, $\left(2\frac{f_0}{f_H}\frac{V}{c}\right)^2$ will generally be very small compared to unity and so the Cerenkov radio emissions will occur.

Under such conditions we adopt the lower frequency of solutions as $f=\frac{f_0^2}{f_H}\left(\frac{V}{c}\right)^2\cos\theta$ ($\theta\neq 0$). In the anisotropic and dispersive medium, the angle between the energy flux direction of the electromagnetic wave and the geomagnetic line of force is generally smaller than that between the wave normal direction and the geomagnetic line of force in the whistler mode (Maeda and Kimura, 1956), and for large values of $\left(\frac{f_0^2}{ff_H}\right)^{1/2}$ that will be generally satisfied in the exosphere, energy flux directions are entirely limited to a cone of semi-angle 19°29′ about the field direction in the whistler mode (Storey 1953).

Therefore the energy of the electromagnetic wave tends to travel in the direction of the particle stream as a result of the guiding action of the geomagnetic field. The condition of the generation of the Cerenkov radiation and the operation of amplification mechanism similar to a travelling-wave tube is given by $V_1\cos\theta=\frac{c}{n}$ and $V_2=\frac{c}{n}$ respectively in the medium of the local refractive index n, where V_1 and V_2 are velocities of protons.

When θ is small but not zero and n is greater than unity, we may consider that Cerenkov radio emissions of the whistler mode are amplified almost simultaneously by the operation of the mechanism similar to a travelling-wave tube due to charged particles different from those causing the Cerenkov radio emissions at different points in space and time. There is lateral stability of the beam when the Maxwell stress tensors of the geomagnetic field exceed the stress tensors of the self-fields and of the beam itself. Neglecting the self-field, this requires that $H^2/4\pi>Nm_iV^2$ where N is the number density and m_i the mass of an ion in the beam, and V is the velocity component parallel to the geomagnetic field H (Harrison 1960).

In the part less than about 4 earth radii from the center of the earth on the

geomagnetic line of force passing through the earth's surface at the geomagnetic latitude of 60°, the above condition is satisfied for auroral particles.

Recently Neufeld (1959) has suggested that an electron beam passing through a dielectric medium may produce an instability that is associated with the growth of longitudinal waves having a velocity close to the velocity of beam and if inhomogeneities are present, these longitudinal waves may be converted into transverse waves and radiated into space at frequencies different from the Cerenkov frequencies, and also Barrington (1959) has suggested the possibility of the coupling between the whistler mode and the space charge modes of an ion stream in the exospheric region considered here. Now assuming that both the Cerenkov radio emissions and the amplification of these waves in a manner similar to the operation of a travelling-wave tube can occur in the exospheric region considered here, we calculate the energy of the Cerenkov radiation due to high speed protons at 2 earth radii from the center of the earth on the geomagnetic line of force passing through the earth's surface at the geomagnetic latitude of 60° where is the most suitable part for above mentioned mechanisms to operate.

The condition for the generation of the Cerenkov radio emissions $\left(V > \frac{c}{n}\right)$ is satisfied at above mentioned part where the electron density is 5×10^3/cm^3, $V=1.4\times10^4$ km/sec, and $n=22.5$ for the radio wave of the whistler mode of which frequency is 5 kc/sec. We have for the total emission in a column of the length of L cm which consists of the high speed protons $S=\frac{4\pi^2e^2}{c^2}\left(1-\frac{1}{\beta^2n^2}\right)\frac{fVNL\times10^4}{10^7}$ watts. m^{-2}. (c/s)$^{-1}$ where N is the number density of protons, V the velocity of protons and $\beta=\frac{V}{c}$ (Shiff, 1949, Marshall, 1956, and Ellis, 1957).

The length of the column is limited within several hundreds kilometers by the frequency bandwidth observed at a moment (Gallet, 1959). Using $\left(1-\frac{1}{\beta^2n^2}\right)\approx1$, $V=1.4\times10^9$ cm/sec, $L=2\times10^7$ cm, $N=10^{-1}$/cm^3, $f=5\times10^3$ c/sec, $e=4.8\times10^{-10}$ e.s.u., and $c=3\times10^{10}$ cm/sec, we have $S=1.4\times10^{-22}$ watts. m^{-2}. $(c/s)^{-1}$.

On the other hand, the incident power flux of dawn chorus recieved at the ground is of the order of 10^{-16} to 10^{-14} watts. m^{-2}. $(c/s)^{-1}$.

Considering that the Cerenkov radio emissions generated by incoming high speed protons are amplified in a manner similar to the operation of a travelling-wave tube and propagate in the whistler mode without a little loss on the way, we can not obtain theoretically the observed power flux of dawn chorus without a gain of amplification greater than 60 *db*. For the physical states existing in the outer ionosphere, in addition to condition of the matching of stream and wave velocities, Bell (1959) has obtained a gain of approximately 2 *db* per wavelength at frequency of 3 kc/sec. This value of gain is very much smaller than we have required.

Concluding Remarks

As we have seen in latitude effect on diurnal maximum of dawn chorus activity,

it is clear that dawn chorus is generated in the earth's exosphere by positively charged particles incoming from the outside of the earth. The most effective radio emissions at frequencies of V.L.F. noise in the exosphere may be the Cerenkov radiation due to high speed protons rather than the proton cyclotron radiation. In order to explain the V.L.F. phenomena, we shall have to consider the generation mechanism of V.L.F. noises and the amplification mechanism of these emissions at the same time in the exosphere. Ellis (1960) has recently reported that bursts of the V.L.F. noise occur even in geomagnetic undisturbed conditions.

It seems likely that hydromagnetic mechanism to accelerate charged particles up to the order of the velocity of 10^4 km/sec and unknown mechanism which frequently causes V.L.F. noises, exsist in the earth's exosphere.

Acknowledgements

The author wishes to express his hearty thanks to prof. Y. Tamura for his kind directions and advices, to prof. K. Maeda, Dr. Y. Inoue, Dr. H. Maeda and Dr. T. Namikawa for their encouragements and supports of this work, and also to Mr. I. Kimura, Dr. H. Matsumoto and Mr. S. Hashizume for their valuable discussions.

References

Allcock G. Mck (1957) Australian J. Phys. **10**, 286.
Barrington R.E. (1959) Proceedings of the Symposium on Physical Processes in the Sun-Earth Environment. Deffence Research Board, Canada. 223.
Bell T.F. and Helliwell R.A. (1959) Proceedings of the Symposium on Physical Processes in the Sun-Earth Environment. Deffence Research Board, Canada. 215.
Ellis G.R.A. (1957) J. Atoms. Terr. Phys. **10**, 302.
Ellis G.R.A. (1959) Planet. Space Science **1**, 256.
Ellis G.R.A. (1960) J. Geophys. Res. **65**, 1705.
Gallet R.M. (1959) Proc. IRE. **47**, 211.
Harrison E.R. (1960) Nature **187**, 383.
Helliwell R.A. (1956) Studies of Low Frequency Propagation. Stanford Univ.
MacArthur J.W. (1959) Phys. Rev. Letters **2**, 491.
Maeda K. and Kimura I. (1956) Rep. Ionos. Res. Japan **10**, 105.
Marshall L. (1956) Astrophys. J. **124**, 469.
Meek J.H. (1955) J. Atmos. Terr. Phys. **6**, 313.
Nagata T. (1949) J. Geomag. Geoelec. **1**, 7.
Neufeld J. (1959) Phys. Rev. **116**, 785.
Ondoh T. and Hashizume S. (1960) J. Geomag. Geoelec. **12**, 32.
Pope J.H. (1957) Nature **180**, 433.
Pope J.H. (1960) Nature **185**, 87.
Shiff L.I. (1949) Quantum Mechanics. McGraw-Hill Co. 261.
Storey L.R.O. (1953) Phil. Trans. Roy. Soc. A **246**, 113.
Veksler V.I. (1957) Atomn. Energ. **2**, 427.
Vestine E.H. (1947) Carnegie Institution of Washington, Pub. No. 580.

Geomagnetic Secular Variation during the Period from 1955 to 1960*

By Takesi NAGATA and Yasuhiko SYONO

Geophysical Institute, University of Tokyo

(Read October 31, 1960; Received December 21, 1960)

Abstract

The isoporic charts of $\dot{X}$, $\dot{Y}$ and $\dot{Z}$ of geomagnetic secular variation during the period from 1955 to 1960 are constructed based on data observed at 99 stations over the earth's surface including the Antarctic region, and illustrated in Figs. 1–9. Equivalent current system of the variation on the earth's core's surface is shown in Figs. 11–13.

From the results of the spherical harmonic analyses of these isoporic charts, it is concluded that (a) the earth's magnetic dipole is decreasing in moment with the rate of -4.4×10^{22} emu/yr, magnitude of the moment at 1960.0 being 8.046×10^{25} emu; (b) the eccentric dipole is drifting westwards by 18′/yr, northwards by 12′/yr, and outwards by $3.4\times10^{-4}\times$ the earth's radius/yr. It is shown that the other harmonics are drifting mostly westwards also with the rate of several decimals of a degree per year.

On the other hand, very intense foci of isopors are found in the Antarctic region, amounting to about 200γ/yr in $\dot{Z}$. The current change on the earth's core's surface equivalent to the foci amount to about 0.1 Amp/cm/yr. This value is strikingly large compared with intensity of the equivalent current of the earth's magnetic dipole, which is about 0.5 Ampere/cm in this region.

1. Introduction

The general features of geomagnetic secular variation during the period from 1950 to 1955 have already been reported on by one of the authors (T.N.) and T. Rikitake[1]. In continuation of the previous report, the general features of geomagnetic secular variation after 1955 will be summarized and analysed in the present report, together with some remarks on the results.

At the request of one of the authors (T.N.), 87 standing magnetic observatories (excluding those in the Antarctic Continent and on some Sub-Antarctic islands) kindly sent him the annual mean values of the geomagnetic three components. In addition to the data from these established magnetic observatories, various information about geomagnetic secular variation in the Antarctic area could be obtained for the period

* Contribution from the Division of Geomagnetism and Planetary Physics, Geophysical Institute, University of Tokyo. Series II, No. 112 (1961)

concerned. It seems that these Antarctic data are quite characteristic in this paper, because geomagnetic isoporic charts covering the whole parts of the earth's surface could be compiled, based on these new data together with those in the other parts of the world.

Thus, the total number of geomagnetic stations, whose data were used in the present work, amounts to 99. The positions of these magnetic stations are listed in Table I, where the periods of observation at each station refered to in the present work are also given, and are shown by full circles in Figs. 3, 8 and 9.

2. Data

At all standing magnetic observatories, including Macquarie Island, Orcadas del Sur and Mawson in the Antarctic region, annual mean values of geomagnetic three components were obtainable. For the purpose of the present work, where the variation during 1955–60 is dealt with, plots of the annual mean values against time at all observatories are classified into three categories, in which the annual rate of the variation has the following tendencies, namely; (a) the annual rate has remained almost constant since 1950 or since the year before; (b) the magnitude of the rate changed more or less around 1955 and has kept nearly constant since then, but the tendency of the variation after 1955 still remains similar to that before 1955; and (c) the annual rate changed its sign after 1955; that is, the plotted curve has a maximum or minimum during the period concerned. Almost all data dealt with here belong to either (a) or (b) category, and only at six stations one of the three components can be classified in (c) category. In Table I, the data of category (b) are marked with a single asterisk (*), and those of category (c) with double asterisks (**), while those of category (a) with no mark.

As for data on categories (a) and (b), there may be no doubts in evaluating the mean annual rate of the variation for the period 1955–60, but there may be some ambiguity in estimating the mean rate for category (c) data. In the present work, however, the simple average of annual rates during the period concerned is adopted as the mean annual rate.

On the other hand, most of the Antarctic stations were operated during IGY or a few years before and after IGY. By examining the monthly mean values, or in some cases the series of the results of absolute measurements, at these Antarctic stations, a fairly reliable value on geomagnetic secular variation could be estimated at 12 stations listed at the bottom of Table I. There are several other stations whose data are not sufficient for determining the secular variation, owing either to the too large effect of polar geomagnetic disturbances or to too short a period of observation.

Since the IGY period was from July 1957 to December 1958, it seems that these data for the IGY period and its extension before and after can show approximately the annual rate of secular variation near the middle period of 1955–60, namely, 1957.5.

Table I. Annual Rate of Secular Variation in the Geomagnetic Field (X, Y, Z) during the Period 1955~60.

CSAGI No.	Observatory	Geographic Lat.	Geographic Long.	Annual rate of Secular Variation $\dot{X}$ (γ/year)	$\dot{Y}$ (γ/year)	$\dot{Z}$ (γ/year)	Period of used data
A021	Thule	76°.5	290°.9	12	13	46	{1947~49 1956~58
A030	Resolute Bay	74.7	265.1	29	7	33	1954~55~58
A031	Bjørnøya	74.5	19.0	9*	20	39	1951~55~58
A039	Point Barrow	71.3	203.3	23	− 4	− 2	1950~55~59
A047	Tromsø	69.7	19.0	8	12	42	1945~55~58
A049	Godhavn	69.2	306.5	19	7	41	1946~55~58
A054	Abisco	68.4	18.8	4*	24	32	1946~50~56
A092	College	64.9	212.2	13	− 4	19*	1948~55~59
A099	Baker Lake	64.3	263.9	30	9	49*	1951~55~59
A121	Srednikan	62.4	152.3	18	−13	17	1946~55~58
A123	Dombas	62.1	9.1	10	20	28	1955~58****
A124	Yakutsk	62.0	129.7	23	−21	13**	1946~55~59
A134	Nurmijärvi	60.5	24.7	1	16	33	1953~55~58
A140	Lerwick	60.1	358.8	17	19	29	1946~55~59
B002	Leningrad	60.0	30.7	5*	10	34	1948~55~59
B009	Lovö	59.4	17.8	4	18	34	1949~55~58
A149	Sitka	57.0	224.7	17	− 7	− 3	1946~55~59
B019	Sverdlovsk	56.7	61.1	6	− 1**	29	1946~55~59
B114	Rude Skov	55.8	12.4	9	22	28	1946~55~59
B028	Kazan	55.8	48.8	− 2	5**	41	1946~55~58
B035	Moscow	55.5	37.3	− 2	6	40	1946~55~59
B038	Eskdalemuir	55.3	356.8	25	27	23	1946~55~59
A154	Meanook	54.6	246.7	32	− 2		1950~54***
B058	Wingst	53.7	9.1	12	27	33	1945~55~59
B071	Witteveen	52.8	6.7	20	27	24	1945~55~59
C362	Irkutsk	52.5	104.0	14	−21	7	1946~55~59
B089	Swider	52.1	21.3	1	21	48	1955~58
B095	Niemegk	52.1	12.7	10	25	32	1945~55~59
B098	Valentia	51.9	349.7	38	25	17	1945~55~59
B114	Abinger	51.2	359.6	27	33	20	1946~55~59 [1]
B119	Hartland	51.0	355.5	32	27	19	1957~59
B132	Manhay	50.3	5.7	17	30	32	1951~55~59
B136	Dourbes	50.1	4.6	21	24	28	1957~59
B143	Průhonice	50.0	14.6	11	27	37	1946~55~59
B163	Fürstenfeldbruck	48.2	11.3	14	32	32	1946~55~58
B172	Hurbanova	47.9	18.2	6	25	40	1949~55~59
C016	Yugno-Sakhalinsk	46.9	142.7	1	−10	−18*	1948~55~58
C018	Odessa	46.8	30.9	− 7*	14	34	1948~55~59
B239	Castellaccio	44.4	8.9	19	38	25	1947~55~59 [2]
C034	Memambetsu	43.9	144.2	3	− 9	−16**	1952~55~59
B249	Agincourt	43.8	280.7	41	−10	3	1950~55~58
C051	Vladivostok	43.1	131.9	7	−11	− 1	1952~55~57 [3]
C364	Tbilisi	42.1	44.7	−12*	− 1*	39	1946~55~59
C076	Tashkent	41.4	69.2	10	−11*	35	1946~55~59
	Istanbul	41.1	29.1	0*	18	61	1949~55~59

Table I. (continued)

CSAGI No.	Observatory	Geographic Lat.	Geographic Long.	Annual rate of Secular Variation $\dot{X}$ (γ/year)	$\dot{Y}$ (γ/year)	$\dot{Z}$ (γ/year)	Period of used data
C093	Coimbra	40.2	351.6	43	43	− 8*	1946～55～59
C098	Toledo	39.9	355.9	35	46	− 3	1947～55～59
B314	Cheltenham	38.7	283.2	38	−14	−20	1946～50～56
B318	Fredericksburg	38.2	282.6	43	−19	−34	1956～59
	San Migule	37.8	334.3	67	30	−39	1947～55～59
C137	Almería	36.9	357.5	42	56	− 5	1955～58
C143	San Fernando	36.5	353.8	44	52		1951～55～59
C147	Kakioka	36.2	140.2	5	− 7	−28*	1946～55～59
	Ksara	33.8	35.9	12	11	63	1945～55～58
C214	Simosato	33.6	135.9	6	− 5	−15	1955～58
C236	Tucson	32.2	249.2	−10	−11	−39	1946～55～59
C251	Quetta	30.2	66.9	9	−16**	19	1954～55～59
C256	Helwan	29.9	31.6	25	24	48	1945～50 1956～58
C273	Tamanrasset	22.8	5.5	32	56	−11	1950～56
C277	Honolulu	21.3	201.9	−23	− 4	−15*	1946～55～59
C287	Teoloyucan	19.8	260.8	− 2	−15	10	1951～53***
	Alibag	18.6	72.9	22	− 6	8*	1947～55～58
C300	San Juan	18.4	293.9	2*	−49	−103	1946～55～59
C311	M'Bour	14.4	343.0	37	61	−67	1952～55～59
E553	Muntinlupa	14.4	121.0	13	−17	−20	1951～55～59
E556	Guam	13.5	144.8	3	6	−26	1957～59
E566	Kodaikanal	10.2	77.5	15	− 5	−22	1950～55～59
E575	Paramaribo	5.8	304.8	−21	−48	−106	1958～59
E583	Bangui	4.6	18.6	22	21	−21	1952 & 1956～59
E590	Tatuoca	− 1.2	311.5	−74	−37	−137	1958～59
E625	Hollandia	− 2.6	140.5	−12	15	−44	1957～59
	Kuyper	− 6.0	106.7	− 6	4**	− 3	1954～55～59
E644	Elisabethville	−11.7	27.5	−35	10	−15	1945～50～55
E646	Huancayo	−12.1	284.7	−54	−60	− 3	1948～55～58
E653	Apia	−13.8	188.2	−20*	11	6	1950～55～59
C901	Tananarive	−18.9	47.5	−25	−18	11	1945～55～59
	Mauritius	−20.1	57.6	−20	−23	−20	1945～55～59[4]
E702	La Quiaca	−22.1	294.4	−59	−57	− 9	1949～50～56
E629	Vassouras	−22.4	316.4	−80	−38	−77	1946～55～58
C925	Watheroo	−30.3	115.9	0	6	−61	1951～55～58[5]
C933	Gnangara	−31.9	116.0	− 4	−14	−36	1958～59
C932	Pilar	−31.7	296.1	−64	−52	8	1949～50～56
C957	Hermanus	−34.4	19.2	−72	26	65	1946～55～59
B966	Toolangi	−37.5	145.5	−19	30	− 5	1949～50～56
B979	Amberley	−43.2	172.7	−28	24	19	1950～55～59
A961	Macquarie Is.	−54.5	159.0	−18	47	16	1952～55～59
A962	Orcadas del Sur	−60.7	315.1	−67	−14	93	1933～55
(Antarctic Region)							
	Heard Is.	−53.0	73.4	−37	−44	−98	1952～54～60 (for X & Y) 1952～54 (for Z)
	Ushuaia	−54.8	251.7	−64	−29	120	1956～58
	Esperanza	−63.4	303.0	−57	−26	107	1956～58
	Merchior	−64.3	297.0	−49	−30	132	1956～58
A973	Argentine Is.	−65.3	295.7	−34	−48	131	1956～58

Table I. (continued)

CSAGI No.	Observatory	Geographic Lat.	Geographic Long.	Annual rate of Secular Variation $\dot{X}$ (γ/year)	$\dot{Y}$ (γ/year)	$\dot{Z}$ (γ/year)	Period of used data
A977	Wilkes	−66.3	110.5	−87	− 1	21	IGY
A978	Mirny	−66.6	93.0	−94	−39	45	1956~58
A980	Mawson	−67.6	62.9	−71	−57	51	1955~58
A984	Syowa	−69.0	39.6	−79	−40	181	1957~59
A989	Halley Bay	−75.5	333.4	−13	−39	70	IGY(6)
A991	Scott Base	−77.9	166.8	−38	15	36	IGY
A995	Little America	−78.3	199.8	7	45	132	IGY

Remarks: * Category (b) in § 2 of the text.
** Category (c) in § 2 of the text.
*** Values before 1955 (for reference).
**** Average for quiet days only.
(1) At Abinger until 1956, and at Hartland since 1957. Data obtained at Hartland since 1957 are reduced to those at Abinger.
(2) Original data are H, D and I.
(3) Data of 1958 and 1959 are ignored, because of their unreasonable discontinuity.
(4) With fair amount of fluctuation on account of some trouble in magnetographs.
(5) At Watheroo until 1958, and at Gnangara since 1958.
(6) This station is built on ice shelf, which is believed to be moving with velocity of 400~600 m/year. Therefore the secular variation values are a little ambiguous.

3. Isoporic Charts $\dot{X}$, $\dot{Y}$ and $\dot{Z}$ for the Period 1955–60

From the above-mentioned data, the mean annual rate of secular variation of the geomagnetic three components X, Y and Z were computed, the results being given in Table I and plotted in Figs. 1~9. In drawing isoporic lines for $\dot{X}$, $\dot{Y}$ and $\dot{Z}$, two basic assumptions were considered; they are (A) that $\dot{\boldsymbol{F}}=(\dot{X}, \dot{Y}, \dot{Z})$ satisfies the conditions, curl $\dot{\boldsymbol{F}}=0$ and div $\dot{\boldsymbol{F}}=0$ near the earth's surface, and consequently $\nabla^2\dot{\boldsymbol{F}}=0$; and (B) that the origin of $\dot{\boldsymbol{F}}$ is situated beneath the earth's surface. In the practical procedure, an isoporic chart for $\dot{Z}$ was first constructed from the distribution of $\dot{Z}$ values with reference to the horizontal vectors $\dot{\boldsymbol{H}}=(\dot{X}, \dot{Y})$, based on the assumptions that div $\dot{\boldsymbol{F}}=0$ and (B), and then isopors for $\dot{X}$ and $\dot{Y}$ were drawn by considering $\partial\dot{X}/\partial y=\partial\dot{Y}/\partial x$. The result of the second process reflects more or less upon the $\dot{Z}$ contours drawn by the first process. Thus, by repeating successively the above-mentioned processes, isoporic charts for $\dot{X}$, $\dot{Y}$ and $\dot{Z}$ satisfying approximately the assumed conditions (A) and (B) were obtained.

On examining Figs. 1–9 in comparison with the corresponding isoporic charts for 1950–55, constructed by Nagata and Rikitake[1], and also with those for 1940–45 by Vestine *et al*[2], it is seen that the general tendency of geomagnetic secular variation over the area from the North pole to 60°S in latitude during the period of 1955–60 was not so much different from those for 1950–55 and 1940–45. Generally speaking, the characteristics of the increase in Z and decrease in X in the southern hemisphere

and the increase in X and rather decrease in Z in the northern hemisphere have been observed during these periods. These characteristics indicate that the decrease in moment of the earth's magnetic dipole, which has been noticed for the past hundred years, was still continuing during the 1950–60 period.

As the present isoporic charts for 1955–60 seem to be more reliable than those for 1950–55, on account of the increase in the number of magnetic observatories, the present charts may be able to be compared with those for 1940–45 in certain details. By comparing these charts for the different periods, the westward drift of the foci of major isoporic vortices in each component can be noticed, the amount of the drift being ranged between 0° and 10° westwards over a period of 15 years. This problem will be discussed in a more analytical way in the following section.

In the isoporic charts around the South pole, illustrated in Figs. 5, 7 and 9, remarkably large values of $\dot{Z}$ over and near the Antarctic may be noticed, amounting to about $2\times10^2\gamma$/year at their maximum. Generally speaking, in comparison with the North polar region, the geomagnetic secular variation is strikingly large and complicated in the South polar region not only for $\dot{Z}$ but also for $\dot{X}$ and $\dot{Y}$, the annual rate of the variation in the latter region amounting to several times more than that in the former region. It has long been noticed that geomagnetic secular variations have been much more active in the Southern hemisphere than in the Northern hemisphere. Even so, it seems that the remarkable secular variation newly found in the Antarctic region is unexpectedly large, and it may need some particular interpretation to explain the existence of such large variations.

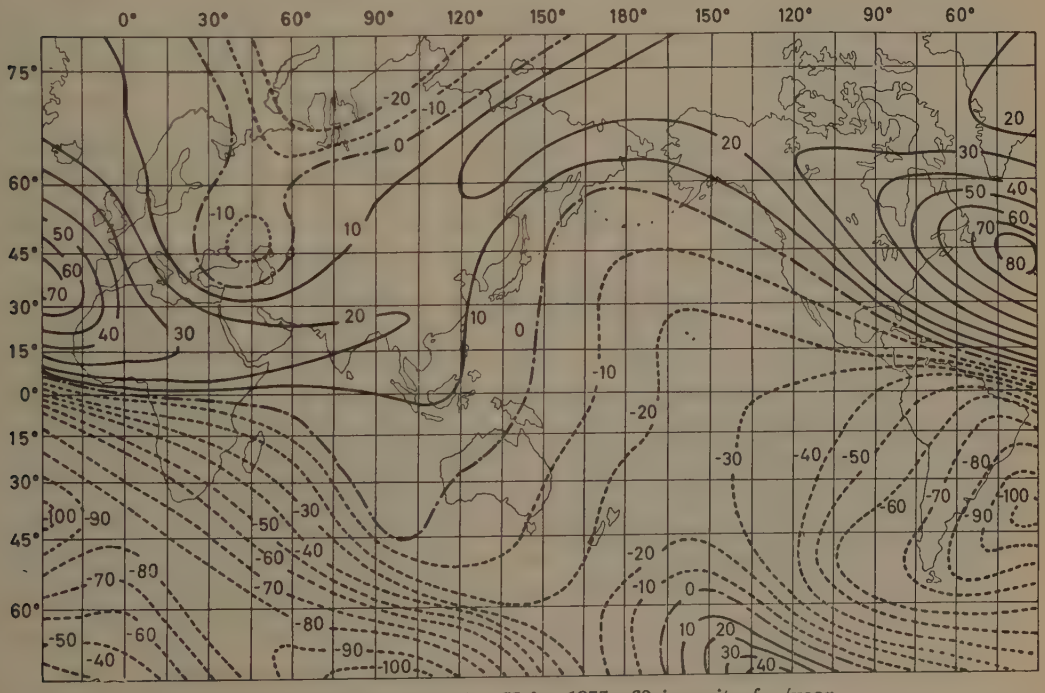

Fig. 1. Isoporic chart for X for 1955~60 in unit of γ/year.

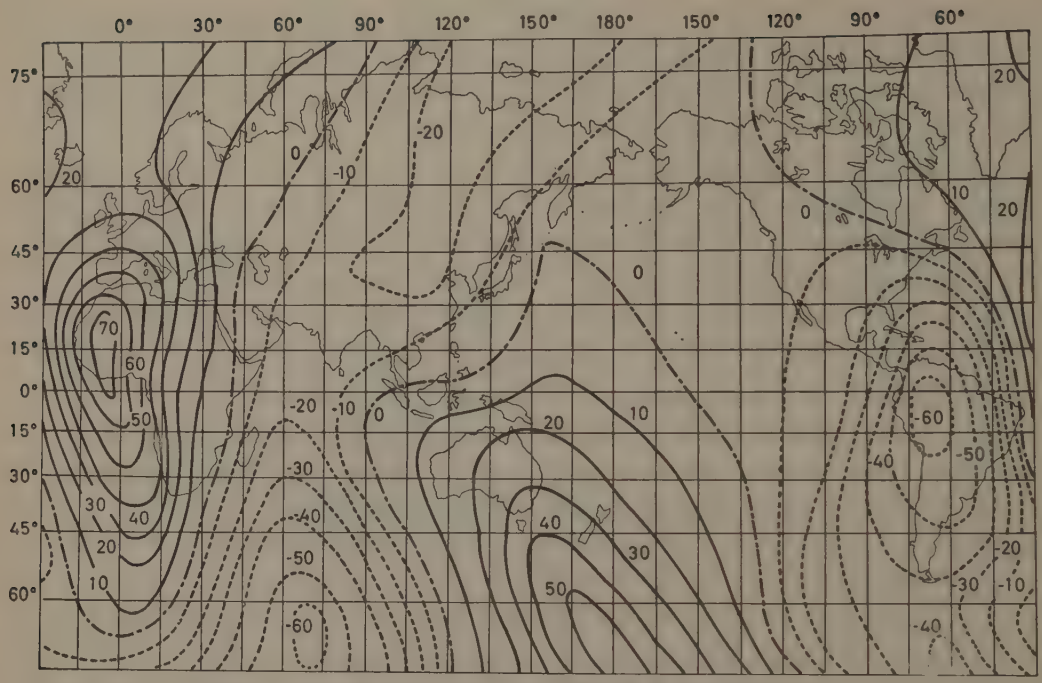

Fig. 2. Isoporic chart for Y for 1955~60 in unit of γ/year.

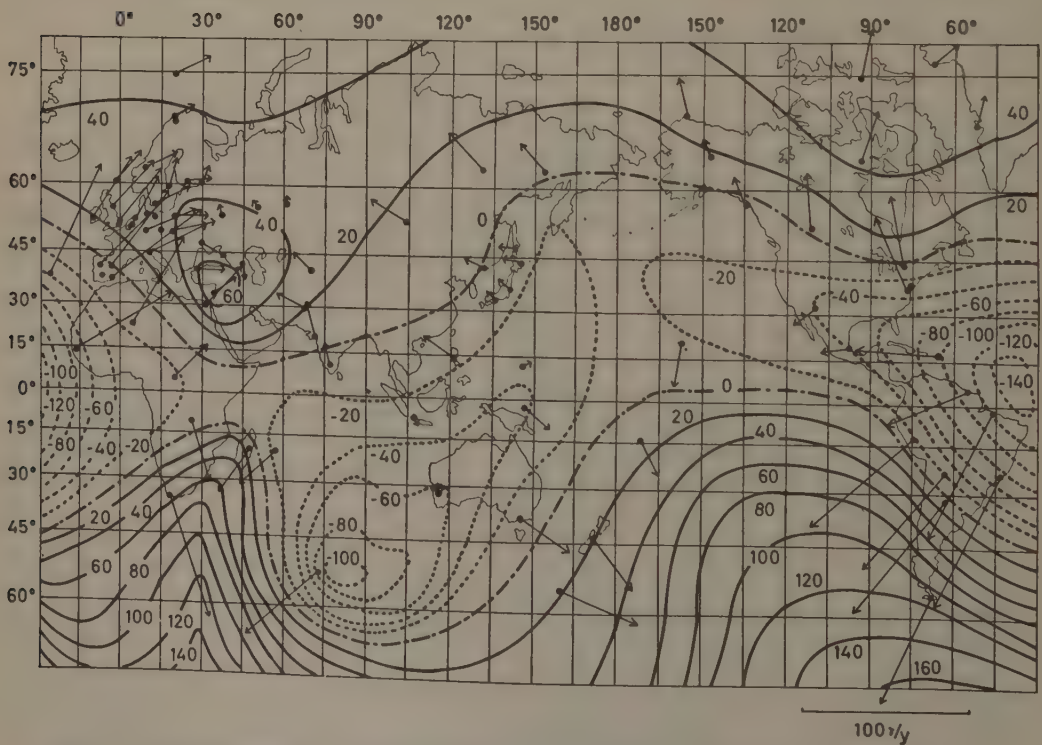

Fig. 3. Isoporic chart for Z for 1955~60 in unit of γ/year. Full circles show the position of observing points and arrows represent $\dot{\boldsymbol{H}}=(\dot{X}, \dot{Y})$.

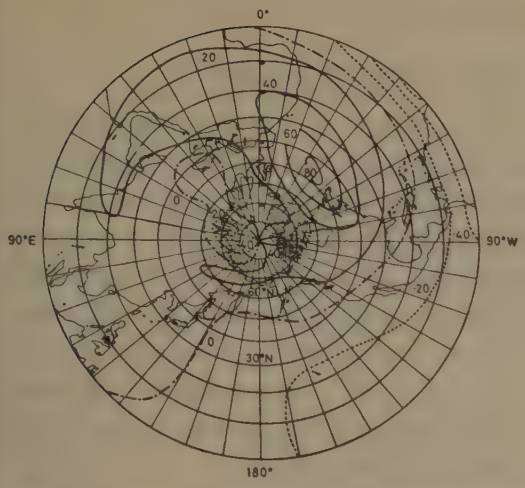

Fig. 4. Isoporic chart for X for 1955~60 in unit of γ/year in the Northern hemisphere.

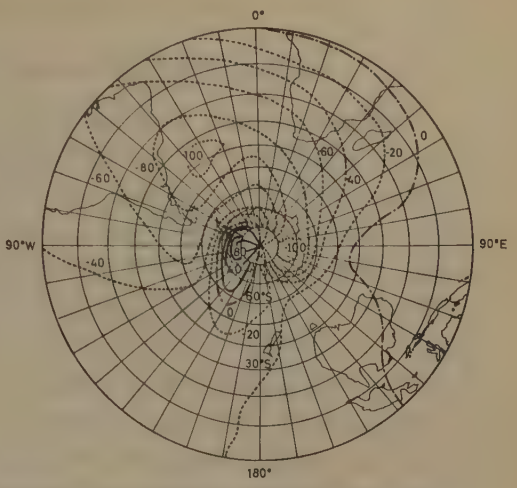

Fig. 5. Isoporic chart for X for 1955~60 in unit of γ/year in the Southern hemisphere.

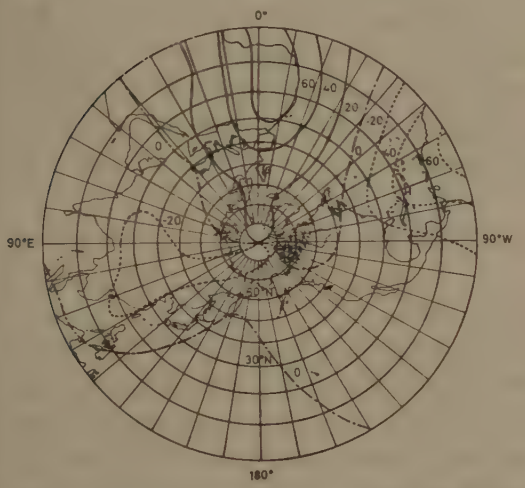

Fig. 6. Isoporic chart for Y for 1955~60 in unit of γ/year in the Northern hemisphere.

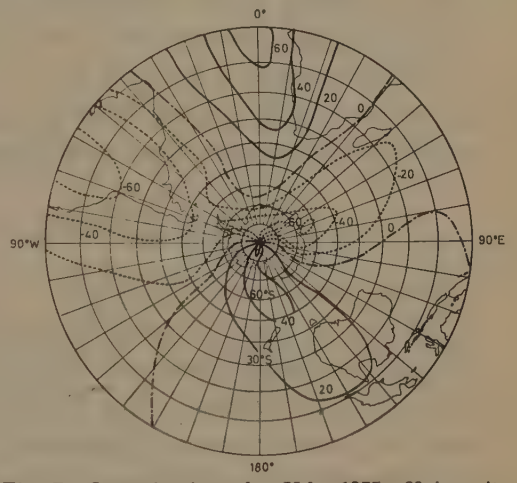

Fig. 7. Isoporic chart for Y for 1955~60 in unit of γ/year in the Southern hemisphere.

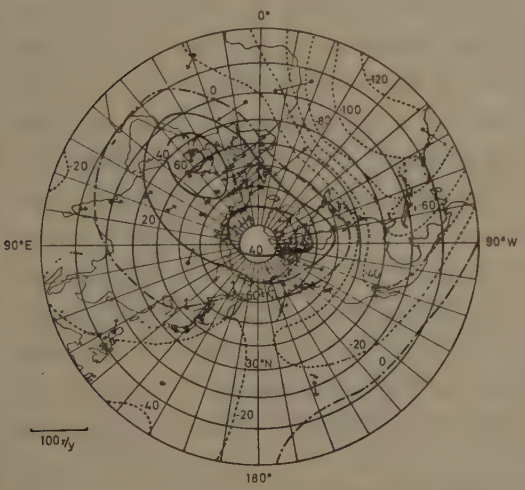

Fig. 8. Isoporic chart for Z for 1955~60 in unit of γ/year in the Northern hemisphere. Full circles show the positions of observing points and arrows represent $\dot{\boldsymbol{H}}=(\dot{X},\ \dot{Y})$.

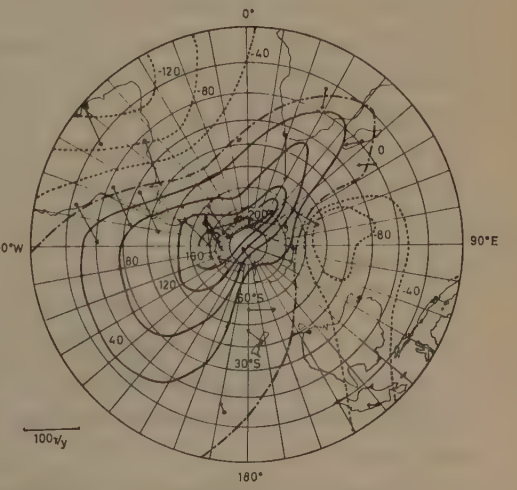

Fig. 9. Isoporic chart for Z for 1955~60 in unit of γ/year in the Southern hemisphere. Full circles show the positions of observing points and arrows represent $\dot{\boldsymbol{H}}=(\dot{X},\ \dot{Y})$.

4. Spherical Harmonic Analysis of $\dot{X}$, $\dot{Y}$ and $\dot{Z}$

The isoporic charts given by Figs. 1–9 were subjected to the ordinary spherical harmonic analyses. In the practical procedures, readings were taken at points every 15° latitude and every 30° longitude in cases where harmonic coefficients up to $n=3$ are evaluated. These analyses were applied to $\dot{X}$, $\dot{Y}$ and $\dot{Z}$ for their distribution within the area between 75°N and 75°S, and also for the area between 60°N and 60°S, the values at latitudes higher than 60° being ignored in the latter case. On the other hand, a more detailed analysis of Z, up to $n=6$, was carried out, based upon the isoporic charts between 80°N and 80°S, in order to obtain an underground equivalent current system in some detail representing the secular variation. In this case, readings were taken at points every 10° latitude and every 15° longitude.

In all cases, results of analyses of the horizontal components, $\dot{X}$ and $\dot{Y}$, were jointed together for determining the coefficients of the spherical harmonic series, while those for $\dot{Z}$ were treated independently of the horizontal components. Results of the above-mentioned analyses are given in Table II, together with those for 1950–55, obtained by Nagata and Rikitake, and for 1910–15, 1920–25, 1930–35, and 1940–45, obtained by Vestine *et al*[2], and in Table III. In these Tables, $\dot{g}_n^m$ and $\dot{h}_n^m$ are defined as usual in the following expression of potential variation; i.e.

$$\dot{V}=R\sum_n\sum_m(\dot{g}_n^m\cos m\lambda+\dot{h}_n^m\sin m\lambda)P_n^m(\cos\theta)\,, \qquad (1)$$

where R denotes the earth's radius.

As will be seen in Table II, it seems likely that the general tendency of geomagnetic secular variations represented by low degree and order harmonic coefficients has been presented nearly identical during the past half century. The main characteristics concerned are (a) decrease in the moment of the earth's magnetic dipole, and (b) westward and northward shift of the position of the eccentric dipole. For the purpose of representing these two characteristics more clearly, moment of the earth's magnetic dipole (M), direction of the centred dipole (co-latitude θ_0 and longitude λ_0 of the North pole of the dipole field), position of the eccentric dipole (latitude φ_M and longitude λ_M and distance r_M from the centre of the earth in unit of the earth's radius R) at the epoch of 1960 were computed, based on (A) 1955 values of the harmonics given by Finch and Leaton[3] and on (B) 1945 values given by Vestine *et al*. In the case of extrapolation from the 1955 values, the present results of secular variation for 1955–60 can be directly applied, while in the case of extrapolation from the 1945 value, the present secular variation data and those for 1950–55 are used. In Table IV, thus estimated values of M, θ_0, λ_0, φ_M, λ_M and r_M/R for cases (A) and (B) are given together with the corresponding values at previous epochs. Now, it may be clear in the above results that M is still decreasing, and the eccentric dipole is drifting northwards, westwards and outwards, while θ_0 has been kept almost constant and the rate of decrease in λ_0 has been rather small.

The speeds of the westward, northward and outerward drift ($-\dot{\lambda}_M$, $\dot{\varphi}_M$, $\dot{r}_M$) of the

Table II. Coefficients of Spherical Harmonic Expansion of Geomagnetic Secular Variations for Various Epochs. (Unit=γ/year)

Coefficients	Author	Vestine *et al*				Nagata-Rikitake		Nagata-Syono			
	Period	1910 –15	1920 –25	1930 –35	1940 –45	1950–55		1955–60			
								75°N–75°S		60°N–60°S	
						X & Y	Z	X & Y	Z	X & Y	Z
g_1^0		25	28	23	9	9	6	15.0	16.0	14.6	12.7
g_1^1		1	4	1	2	0	2	12.0	6.4	11.4	6.6
h_1^1		− 7	− 7	− 5	1	4	− 1	− 2.0	1.3	− 4.1	1.1
g_2^0		− 7	−10	−14	−18	−25	− 8	−22.3	−25.3	−20.7	−22.0
g_2^1		− 1	1	1	0	0	− 1	− 2.6	− 1.0	− 2.7	− 1.7
h_2^1		− 9	−14	−18	−20	−17	−16	−18.0	−17.5	−13.6	−17.0
g_2^2		24	17	10	2	4	− 3	0.0	− 0.3	− 0.2	− 0.4
h_2^2		−17	−17	−14	−14	−14	−11	−16.8	−17.9	−16.3	−17.8
g_3^0		6	7	4	2	6	− 2	1.0	− 0.9	1.3	0.7
g_3^1		− 6	− 7	− 7	7	0	− 3	− 9.8	− 9.2	−13.2	− 7.9
h_3^1		− 6	− 5	− 5	− 1	0	3	7.4	8.4	5.9	7.8
g_3^2		− 1	− 2	−1	3	1	2	1.3	0.7	1.1	0.8
h_3^2		3	3	4	4	7	− 1	1.5	4.3	1.2	4.1
g_3^3		13	7	3	0	− 1	− 6	− 1.4	− 2.0	− 1.3	− 2.0
h_3^3		−11	−11	−13	−10	− 8	− 2	− 7.7	− 5.8	− 7.6	− 5.8

Table III. Coefficients of Spherical Harmonic Expansion of $\dot{Z}$ during 1955–60. (Unit=γ/year)

$[\dot{g}_n^m]$

n \ m	0	1	2	3	4	5	6
1	13.6	5.9					
2	−21.5	−1.8	−0.1				
3	1.9	−8.2	1.1	−0.5			
4	− 4.4	2.7	−2.0	−1.0	−2.2		
5	2.1	−1.8	0.2	1.0	−0.5	−0.2	
6	− 1.7	2.1	0.1	−0.3	1.5	0.5	−0.6

$[\dot{h}_n^m]$

n \ m		1	2	3	4	5	6
1		2.3					
2		−16.0	−17.1				
3		8.2	3.5	−6.7			
4		0.0	− 1.1	3.5	−2.1		
5		1.8	1.7	−3.8	0.7	0.2	
6		− 0.7	− 0.2	1.5	−1.1	0.7	1.0

Table IV.

Epoch	Author of analyzed data	M	θ_0	λ_0	φ_M	λ_M	r_M/R
		emu					
1885	Schmidt[4]	8.346×10^{25}	11°28′	291°30′	5°36′N	168°12′	0.0461
1922	Dyson-Furner[4]	8.169 ,,	11 34	290 54	9 13	161 16	0.0570
1945	Vestine *et al*[2]	8.082 ,,	11 24	289 54	13 56	154 05	0.0630
1955	Finch-Leaton[3]	8.068 ,,	11 42	291 03	15 41	150 49	0.0685
1960(A)	Extrapolated from F-L 1955 values	8.046 ,,	11 30	290 34	16 40	149 20	0.0702
1960(B)	Extrapolated from Vestine's 1945 values	8.025 ,,	11 40	289 16	17 21	149 08	0.0679

Table V.

	Average for 1955–60	Average for 1945–60	Average for 1922–55
$-\dot{\lambda}_M$	+18′/yr	+20′/yr	+19′/yr
$\dot{\varphi}_M$	+12′/yr	+14′/yr	+12′/yr
$\dot{r}_M/R$	$+3.4\times10^{-4}$/yr	$+3.2\times10^{-4}$/yr	$+3.5\times10^{-4}$/yr
$\dot{M}$	-4.4×10^{22}emu/yr	-3.8×10^{22}emu/yr	-3.1×10^{22}emu/yr

eccentric dipole and the annual rate of change in the dipole moment ($\dot{M}$) are estimated as given in Table V. So far as the rate of secular change in moment M and that of the drift of the eccentric dipole during recent years are concerned, it seems likely that those values estimated directly from the secular variation data obtained at a number of geomagnetic observatories may be more reliable than those estimated from the difference between magnetic charts at different epochs, which are compiled by different authors with different methods.

As for the drift of the geomagnetic non-dipole field along latitude circles, each

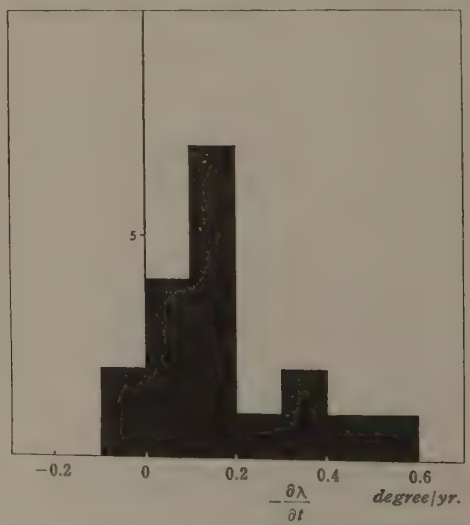

Fig. 10 Histogram of drift velocity of spherical harmonics ($2\leq n\leq 4$) of the geomagnetic secular variation along latitude circles.

spherical harmonic term (g_n^m, h_n^m) of secular variation distribution can be examined directly. If the non-dipole field potential represented by

$$W=R\sum_{n=2}^{\infty}\sum_{m=0}^{n}(g_n^m\cos m\lambda+h_n^m\sin m\lambda)P_n^m(\cos\theta)\,, \qquad (2)$$

has been drifting along latitude circles without changing its distribution form, its change is given by

$$\dot{V}=\frac{\partial V}{\partial\lambda}\cdot\frac{\partial\lambda}{\partial t}=R\sum_{n=0}^{\infty}\sum_{m=0}^{n}m[h_n^m\cos m\lambda-g_n^m\sin m\lambda]\frac{\partial\lambda}{\partial t}\cdot P_n^m(\cos\theta)\,, \qquad (3)$$

where $\partial\lambda/\partial t$ gives the velocity of the westward drift. Then, from (1) and (3), we get

$$\text{Westward-drift velocity}=\frac{\partial\lambda}{\partial t}=\frac{\dot{g}_n^m}{mh_n^m}=-\frac{\dot{h}_n^m}{mg_n^m}\,. \qquad (4)$$

From the values of ($\dot{g}_n^m$, $\dot{h}_n^m$) given in Table III, and the values of (g_n^m, h_n^m) for 1950 obtained by Finch and Leaton, numerical values of $\partial\lambda/\partial t$ were computed for 18 couples of coefficients for $4\geqq n\geqq 2$. The results are shown in Fig. 10, as a histogram of $\partial\lambda/\partial t$ values. It may be seen in this diagram that each of the harmonics is drifting mostly westwards with a velocity of several decimals of a degree per year.

5. Equivalent Current System of Geomagnetic Secular Variation over the Surface of the Earth's Core.

From the harmonic coefficients, $\dot{g}_n^m$ and $\dot{h}_n^m$, for $n\leqq 6$, given in Table III, the equivalent current system on the surface of the earth's core, namely on the spherical surface of 2900 km in depth from the earth's surface, can be obtained. Figs. 11–13 illustrate the distribution of the equivalent current system, where the harmonic coefficients $n\geqq 7$ are ignored.

It seems that the distribution of secular variation can well be represented by the equivalent current system of $n\leqq 6$ over almost all regions over the earth except the Antarctic region. As already mentioned, regional anomalous variation around the south pole is extremely large and local, so that a difference (observed value minus computed value by this equivalent system) still amounts to from -40γ/yr to 40γ/yr for $\dot{Z}$ in this Antarctic region. Attention may be especially paid to a pair of $\dot{Z}$ foci in the vicinity of East Antarctica, a positive $\dot{Z}$ focus on inland in East Antarctica and a negative $\dot{Z}$ focus near Heard Island, the distance between them along the great circle and the difference between their Z foci is the result of a pair of radial magnetic dipoles on the earth core's surface, the position and intensity of these dipoles are estimated as illustrated in Fig. 14, which shows a cross section of the earth along the great circle passing through these foci.

As shown in the figure, the upward magnetic dipole has about 3.5×10^{22}emu/yr in its annual rate of change in moment, while the downward one about 15° apart is about 2/3 in its change of moment. The two curves of the upper half of the figure illustrate the distribution of $\dot{Z}$ and $\dot{H}$ derived from the pair of dipoles and the circles represent the corresponding observed values at the four stations. The above-mentioned result may indicate that a change in electric currents of the form of a pair of vortices, one

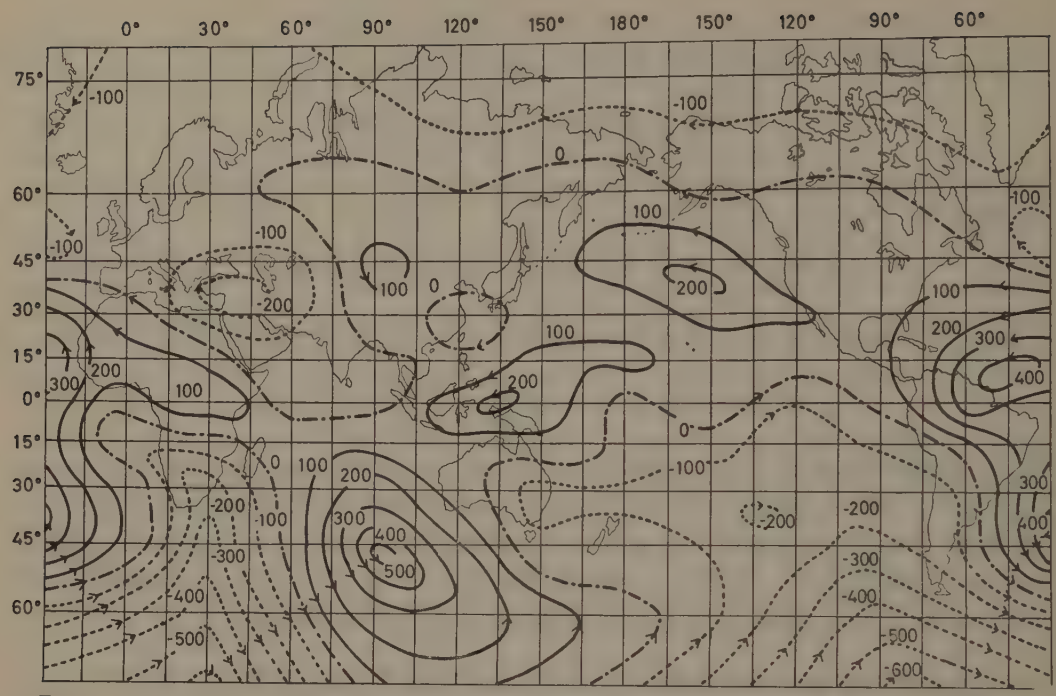

Fig. 11. Equivalent current system of the geomagnetic secular variation at depth of 2900 km in unit of 10^4 Ampere/year.

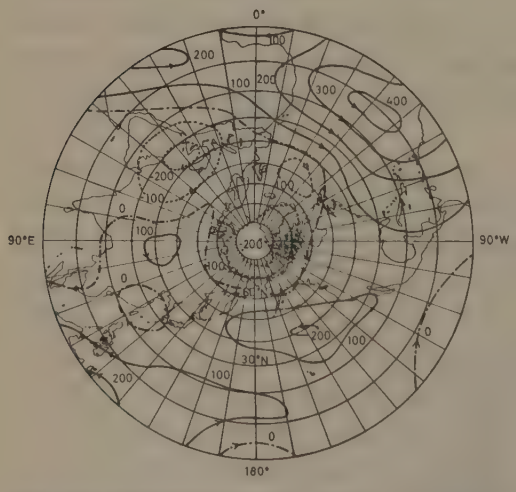

Fig. 12. Equivalent current system of the geomagnetic secular variation in the Northern hemisphere at depth of 2900 km in unit of 10^4 Ampere/year.

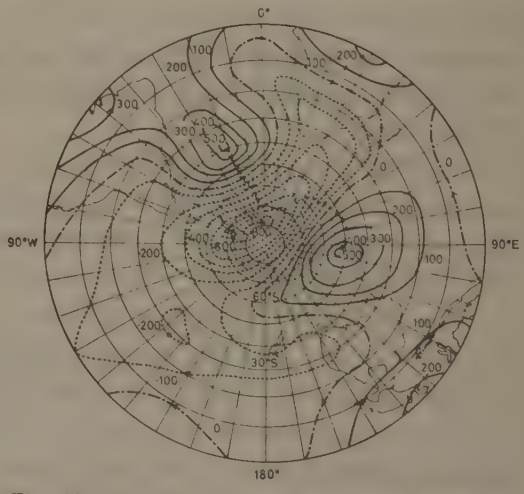

Fig. 13. Equivalent current system of the geomagnetic secular variation in the Southern hemisphere at depth of 2900 km in unit of 10^4 Ampere/year.

clockwise and another counter-clockwise, is taking place near the core's surface beneath this region. This means that equivalent currents between the two foci of vortices on the core's surface are changing at the rate of about 0.1 Amp/cm/yr. (In Fig. 13, concerned only with lower spherical harmonics of $n \leqq 6$, the rate of change in electric current density amounts to about 0.05 Amp/cm/yr.) It may be said that this rate of change

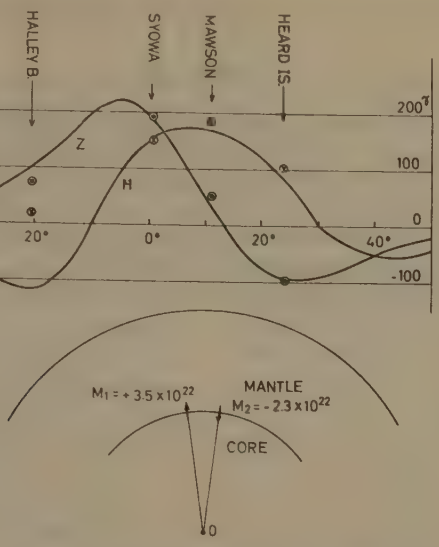

Fig. 14. Distribution of $\dot{Z}$ and $\dot{H}$ along the great circle plane passing through Syowa and Heard Island in the Antarctica.
Above: observed values of $\dot{Z}$ and $\dot{H}$ and those produced by a pair of magnetic dipoles illustrated below.

in electric currents is significant, compared with the equivalent current of the earth's main dipole field.

Intensity of electric currents over the core's surface, equivalent to the earth's dipole field, is approximately given by $I_0=1.4\cos\varphi_m$ Ampere/cm, where φ_m denotes geomagnetic latitude, and therefore their intensity in this region where $\varphi_m\approx 60\sim 70°$ is about 0.5 Ampere/cm or less. Then, the total amount of current change of the vortex-form in the Antarctic area over several years ought to become as extensive as the intensity of the dipole-field current. On the other hand, observed evidence has shown that the large rate of geomagnetic secular variation in this area has continued throughout the past 30 years, at least[5].

It seems unlikely therefore that the intense regional secular variation of a pair of vortex represents in form the simple fluctuations in the electric current system within the core responsible for the geomagnetic dipole field owing to its instability. Alternatively, it might be rather reasonable to presume that the change is caused by the breaking out of a part of the inner toroidal magnetic field, such as is assumed by Bullard[6], or by the flowing up and breaking out of a ring of the toroidal magnetic field near the core's surface, such as is assumed by Alfvén[7] in explaining a pair magnetic field of the sunspots.

Acknowledgement

The present work was carried out as part of the scientific activities of the Committee on Secular Variation and Palaeomagnetism of the International Association of Geomagnetism and Aeronomy. The authors are grateful to all members of the magne-

tic observatories listed in Table I, who kindly placed geomagnetic data at their disposal.

References

(1) Nagata, T. and Rikitake, T., Journ. Geomag. Geoelec., **9**, 42 (1957)
(2) Vestine, E.H. *et al*, Carnegie Inst. Washington Publ., No. 580 (1947)
(3) Finch, H.F. and Leaton, B.R., M.N.R.A.S., Geophys. Suppl., **7**, 314 (1957)
(4) Fanselau, G., "Geomagnetismus und Aeronomie", Bd. III, p. 203 (Berlin, 1959)
(5) Nagata, T., Oguti, T. and Kakinuma, S., Proc. Japan Acad., **34**, 427 (1958)
(6) Bullard, E.C., M.N.R.A.S., Geophys. Suppl., 5, 248 (1948)
(7) Alfvén, H.. "Cosmical Electrodynamics", pp. 116–145 (Oxford, 1950)

Abstracts of the Papers Presented at the 28 th Annual Meeting, Kyoto, Oct. 30–Nov. 1, 1960.

OGAWA T. and SAGA S. (Geophysical Institute, Kyoto University) **Charge on Rain Drop (Continued report)**——The problem on the electricity of precipitation is to search the electric charge on rain drop for the history of charging. This paper is our primary attempt to know the magnitude of the original charge on rain drop by considering the rain current at the ground on the standpoint of Wilson's ion-capture theory. In general, the rain current is represented by the equation $i=\int_0^\infty NQVdx$, where N is the size distribution of rain drops, Q the charge and V the falling velocity of a rain drop. All of these variables are the functions of drop size x. If the charge on rain drop can be negligible small compared with $3Xa^2$ (X: the electric field in esu, a: the radius of rain drop in cm) at any instant during the time interval in which the rain drop falls from a cloud to the ground, the charging rate of rain drop is represented by $dQ/dt=-3\pi\lambda Xa^2$ according to the calculation of Whipple and Chalmers, where λ is the polar conductivity in esu. Applying the result of integration of this equation to the rain current, we tried to dissect Simpson's empirical formula. As the result of this dissection, a relation of $n\simeq 695\lambda$ is obtained, assuming the original charge on rain drop $Q_0=3nXa^2$. The relation is given in the following table for some values of λ.

λ (esu)	n
1.5×10^{-5} (Average value at Kew)	0.0104
1×10^{-4} (Average value at land stations)	0.0695
2×10^{-4}	0.139

Thus rain drop starts a cloud with a small charge compared with $3Xa^2$ in the same sign as the electric field, and reverses its sign during the fall to the ground. As n must be a certain definite value, the process in which the charge on rain drop changes its sign in the region below cloud proceeds depending on the value of conductivity; this may be the reason why the mirror image effect has been found clearly at some stations and not so at others.

SAGA S. and OGAWA T. (Geophysical Institute, Kyoto University) **Electric Field below Cloud**——On the disussion of the charge on rain drop, there remains a serious problem on the electric field below the cloud, that is the discrepancy between the Altielectrograph results by Simpson and Scrase and Simpson and Robinson, and theoretical calculation by Whipple and Scrase on the basis of Wilson's Space Charge Theory. Taking the life time of small ions into the consideration, the authors found the possibility of rapid increase of the field below the level of 100 m; the magnitude at the level of 100 m is about ten times as large as that at the ground. This rapid increase may have caused the erroneous estimation of the coefficient in the relation between the current and the field strength used by Simpson and Scrase, and so the above discrepancy may have arisen. Standing on this supposition, the small ions produced by point discharge do not ascent above the height of a few hundred meter, and the electric field remains nearly constant above that level. Consequently it may be thought on Wilson's process below the cloud, that the rain drop captures hardly ions produced by point discharge, but mainly small ions which contribute to the normal conduction current under the high electric field.

MISAKI M. (Meteorological Research Institute) **Studies on the Atmospheric Ion Spectrum II**——In the previous investigation on the mobility spectrum of atmospheric ions with mobilities greater than 0.4 cm²/volt sec, it was deduced that small ion concentration was too small to account for the electrical conductivity, so that we were forced to conclude that there might be appreciable contribution of large ions to conductivity. This is likely to occure when the air is polluted as in the case of the large city. To leave little room for doubt about this, however, we must further proceed with the studies on the spectrum in the region smaller than 0.4 cm²/volt sec. A thick probe, 12 cm in diameter, was produced for the measurement of spectrum in the mobility region down to 0.002 cm²/volt sec. This probe has the same length

with the slender one for small ions, and can be replaced with it into the aspiration cylinder. In the present works, spectra were obtained between 0.4 and 0.02 cm^2/volt sec. Analysis of several examples showed that the contribution of large and intermediate ions to the conductivity attains to a few tens percent of total conductivity. This is in agreement with the postulate of previous works.

UCHIKAWA K. (Japan Meteorological Agency) **On the Atmospheric Electric Phenomena in the Upper Air (Variations in the Vicinity of Exchange Layer)**——Measurements of electrical conductivity and potential gradient in the upper air using special designed radiosondes were carried out at four stations in Japan (Sapporo, Tateno, Hachijojima and Kagoshima) during IGY and IGC. An investigation of these results shows that height of the exchange layer has its mean value of 2200 m, and varies slightly from season to season, showing high in summer and low in winter. Considerable discontinuities of columner resistance and space charge are observed at the boundary between the exchange layer and the upper level. This discontinuity, however, disappears when meteorological disturbances (cyclone, front etc) pass through the observation point, and then continuous distributions of these elements last for several days. Calculating from observed values of temperature and wind at the level of the boundary, descending current (or ascending current) is presumed when the exchange layer exist (or not).

TAKAGI M. (The Research Institute of Atmospherics, Nagoya University) **On the Discharges in the Thundercloud.**——The discharge in the thundercloud is composed of a main slow discharge process and of many rapid local breakdowns occurring in a slow discharge process. The investigation of the polarities of electro-static field changes and of the amplitude relations between static field changes and light emissions, both produced by such local breakdowns, has led to the following results. The cloud discharge is generally produced between the main upper positive and lower negative charged regions in the thundercloud, and the successive positions of local breakdowns are descended with the downward development of a slow main discharge process started from the positive charged region, but a local breakdown is accomplished in itself by the negative short streamer advancing rapidly upward. While the discharge inside the cloud, appearing between and after the multiple ground strokes, is similarly constructed by a slow positive discharge process and rapid negative local streamers, excepting that the directions of advances are respectively contrary with those of the cloud discharge.

TAKEUTI T. and ISIKAWA H. (The Research Institute of Atmospherics, Nagoya University) **Ground Discharge Mechanism Deduced from Electric Field Records Obtained Simultaneously at Two Places.**——From electric field records obtained at Maebashi and Shibukawa, which is north apart 13 km from the former, two results about ground discharge are obtained. (1) We obtained a few couples of electric field change records by cloud discharges preceding the first ground strokes, which is named pre-preliminary discharge in our paper.* As the number of records is too poor to discuss about it, we only show those records. (2) It has reported that ground strokes neutralize successively upward a negative charged column in a thunder cloud. We have deduced that the negative charged column inclines, so that the stroke pass in the cloud has horizontal direction component, and the J and F processes named by Malan also have horizontal direction component. *Takeuti T. etc. Proc. Res. Inst. Atmo. vol. 7 p. 1 1960.

ISIKAWA H. (The Research Institute of Atmospherics, Nagoya University) **The Interpretation of the Pulsive Structure of the Electromagnetic Waveform of a Preliminary Discharge**——The time intervals between radiation pulses appearing on the waveform of a preliminary discharge have been measured on electromagnetic waveforms. The variation of time intervals between appreciable pulses with the progress of a preliminary discharge measured on the waveforms fairly well coincides with the step interval variation with the progress of a stepped leader measured on the photographs of stepped leaders. Numerous small pulsations superposed on a series of appreciable amplitude pulses, however, usually have the frequency of repetition more than 50 kc and can not be considered to correspond each to a step streamer. The variations of pulse intervals with the discharge progression have been compared between α type and β type stepped leaders, however, we can not find any essential difference existing between the two. The difficulty in photographing a clear β type stepped leader

therefore should be attributed to the decrease in the streamer luminosities.

TUKIZI O. (Electrical Communication Laboratory, Nippon Telegraph and Telephone Public Corporation). **Unified Theory for Tropospheric Propagation of Radio Waves** ——A theory of radio propagation in a homogeneous atmosphere valid for all regions within, near and beyond the radio horizon is presented. Use of the saddlepoint method which proves useful for analysis of the normal propagation within the horizon reduces the problem to finding an appropriate root of the saddle-point equation. It is found that the magnitude of this root is closely related to the field strength received at a distance from the transmitter and that its imagi nary part, in particular, determines the nature of the received field strength which varies markedly from a region to another. Dependence of the received field strength on the gradient of atmospheric refractive index near the earth surface is discussed.

MIYA K. (Kokusai Denshin Denwa Co., Tokyo) **Bearings of Atmospherics at HF**——Bearings of atmospherics at 5, 10 and 15 Mc/s were measured at Ohira near Tokyo in December, 1955, by using a direct vision type direction finder. Ranges of bearings were obtained from a photograph taken with 1 minute exposure. Atmospherics generally arrive from a wide range of southerly bearings except a range between 320° and 50°. Atmospherics at 5 and 10 Mc/s change their bearings clockwise, i.e. from south to northwest in the morning and from northeast to south in the afternoon. On the other hand, atmospherics at 15 Mc/s almost arrive from southerly bearings throughout a day. The above characteristics of bearings are explained by differences of strengths of atmospherics induced in beam antennas pointing to different directions of 53°, 244° and 337°. It is shown that these results can be well explained by using the worldwide mop of atmospherics, which is rearranged from the maps of CCIR report, in the expression of U.T.

TSUBOKAWA I., FUJITA N. and SETO T. (Geographical Survey Institute) **On Proton Precession Magnetometer (Comparison with G.S.I. Magnetometer)**——The component proton precession magnetometers reported by Tsubokawa I. in 1957, are now being operated in the Kanōzan Geodetic Observatory, recording H and F continueously (recording speed: 50 mm/h, sensitivity: about 1 mm/γ, time interval: 30 sec.). The head of the magnetometer for H is placed in the field of Fanselau coil whose current is regulated in the accuracy of 0.5 % automatically. The coil axis error and the level error are being checked and corrected once a week. The dip computed from the records of F and H of proton precession magnetometer are compared with that obtained directly by G.S.I. magnetometers No. 27 and No. 41 which are electromagnetic magnetometers with rotating coil detector. These instruments are respectively placed in different stations. The difference of the geomagnetic field among the stations where the proton precession magnetometers and G.S.I. magnetometers are placed, are determined by above mentioned G.S.I. magnetometers, exchanging them alternately. The result is as follows:

$$I_P - I_G = 0.'00 \pm 0.'03$$

Where I_P is the dip computed by the proton precession magnetometers and I_G is the dip obtained by G.S.I. magnetometers. This shows I_P and I_G agree with each other within the accuracy of observation.

KATO Y. and Other Members of Research Group of Air borne Magnetometer (Geophysical Institute, Tohoku University) **On the Air-Borne Magnetometer (For the Measurement of the Vertical Component**——We constructed the new type air-borne magnetometer for the direct measurement of the vertical component of the earth magnetic field. The detector core of this magnetometer is fixed on a vertical air-gyroscope which holds the vertical direction by means of high speed rotation. The method of measurement of the vertical component of the earth's magnetic field is an application of the Tohoku University Method for the measurement of the week magnetic field and one kind of so-called saturable core magnetometer. The magnetic core of easily saturable ferromagnetic material of high permeability is set on the vertical axis of revolving body of the gyroscope, and the primary and secondary coils are set on the bracket of the gimbal (on which the gyroscope is mounted). The rotating body of gyroscope having a large angular momentum does not make any change evenwhen the gimbal

receive some acceleration in a short time. Thus the axis of the gyroscope or the magnetic core of the magnetometer hold the vertical direction, and we can detect the vertical component of the earth magnetic field in the airplane. We could observed the magnetic anomaly above 3000 m of Mt. Mihara, Ooshima and we could separate the magnetic anomaly due to the subterranean structure of the Mt. Mihara and the basement structure of Ooshima.

HARADA Y. (Geographical Survey Institute) **Geomagnetic Anomaly Distribution in Japan**——From the results of the second order magnetic survey at about 800 stations established during the periods from 1952 to 1959 in Japan, magnetic charts of three components for 1955.0 are obtained. Method of the least square with a condition equation, rot H=O, is used for the seven sectorial zones independently, and then magnetic chart is combined from the seven partial charts. A) From the main distribution represented by second order polynomial equations, two anomalous zones for Y-component are found along Fuji volcanic range in Honsyu and Hidaka Mt. range in Hokkaido. The magnitudes of the anomalies are estimated to about 20' in declination. B) From the residual charts, (a) positive anomalies of Δz are found in alluvium and pleistocene districts; (b) negative anomalies of Δz are found in the mountaineous districts, Chubu, Shikoku, Chugoku and Kyushu; (c) large positive anomalies in Δz over than 200γ along the volcanic ranges are remarkably found; (d) generally speaking, Western Japan is not so much disturbed, while Eastern Japan is much disturbed.

YUKUTAKE T. (Earthquake Research Institute, Tokyo University) **Preliminary Study on the Secular Variation of the Geomagnetic Field**——Time variation of the magnetic field at the earth's surface consists of two different kinds of variation; one originated in the steady movement of the field and other caused by the growth or decay of the drifting field. Some trials to evaluate their contributions to the field variation have been commenced. Spectrum analysis of the varying magnetic field based on palaeomagnetic investigations showed that phenomena having such periods as 7000, 3000, 1800, 1200, 800 and 400 years were conspicuous. The most of these rather seem to be associated with the drift of the main features of the field at the earth's surface than the variation related to the vissicitude of the fluidal motion in the core. Analysis for short intervals of recent observations revealed the 50- and 25-year period, though whether these originate within the earth or not is unknown yet. Assuming that the centered dipole has shown no appreciable movement over thousand years, the variations in declination and inclination caused by the steady westward drift of the non-dipole field were constructed for last one thousand years in Japan and compared with archaeomagnetic results. Good correspondence can be seen regarding the main features of variation when drift velocity of about 0.35°/year is assumed. The same kind of comparisons suggest that the drift velocity in the past might be faster than now.

NAGATA T. and SYONO Y. (Geophysical Institute, University of Tokyo) **Geomagnetic Secular Variation during 1955-60**——Geomagnetic isoporic charts of X, Y and Z for the period of 1955-60 were constructed, based upon observed data at 99 stations including 12 Antarctic ones. The results were subjected to spherical harmonic analysis. Main points of the results are as follows.

(a) Moment of the earth's magnetic dipole has continued to decrease. The values of the moment (M) and position (φ_0, λ_0) of north pole of the dipole at 1960.0 are:—

M (1960)$=8.046\times10^{25}$ emu,

$\varphi_0(1960)=78°30'N$, $\lambda_0(1960)=290°34'$.

(b) The geomagnetic eccentric dipole has continued to drift westwards, northwards and outwards. The position (Lat.$=\varphi_M$, Long.$=\lambda_M$, distance r_M from the earth's centre in unit of the earth's radius R) of the eccentric dipole at 1960.0 are:—

$\varphi_M=16°40'N$, $\lambda_M=149°20'$, $r/R=0.0702$,

while its velocity of drift is given by

$\dot{\varphi}_M=+12'/yr$, $\dot{\lambda}_M=-18'/yr$,

$\dot{r}_M=+3.0\times10^{-4}R/yr$.

(c) Velocity (Λ) of the westward drift was estimated by

$\Lambda=-\dot{g}/mh$ and $\Lambda=+\dot{h}/mg$ for harmonics of $m\leqq n\leqq3$. Average of Λ values is $-15'/yr$.

(d) There is a twin of extremely intense positive and negative foci of $\dot{Z}$ near the coast of East Antarctic. There intensity amounts to about 200 γ/yr.

KONDO I., MURAYAMA T., MORI S., OKADA H., MAKINO T., SAKAKIBARA S., KATO S and HONZAWA T. (Physical Institute, Nagoya University) **On the Observation of High Energy Cosmic Ray Particles by Cosmic-Ray Telescope No. 3 (I) Detection Efficiency**——Calculations were made on the detection efficiency of cosmic ray particles for newly built Cosmic-Ray Telescope No. 3 (J. G.G. 12, 46, 1960). (1) Maximum number of photo-electrons available at the photo-cathode of multiplier photo-tubes was determined as 34 for each passage of a particle, including the effect of the wave length shifter (n_t=34). (2) To suppress accidental coincidences to several counts per hour, photo-tube pulses are discriminated at such a pulse height that corresponds to 1.5 electrons at the photo-cathode (n_b=1.5). (3) With above mentioned values of n_t and n_b, the solid angle for each four-fold coincidence can be estimated to be $4° \times 6°$, and about 7° in diameter for a "*Y*-element" (mixture of three 4-*f* coincidences). The total field of view is about 17° in diameter which consists of six "*Y*-elements" and six "*V*-elements" (mixture of two 4-*f* coincidences). As these elements overlap one another, incoming particles are detected with high efficiency (>95%) in this field view. (4) The effective area of the telescope is about 10 m². (5) Expected intensity of vertical cosmic rays to be observed by this telescope is estimated with the knowledge on the energy spectrum of vertical μ-mesons and electrons, amount of Čerenkov light as a function of a particle velocity and the geometry of the telescope (shown in (3) and (4)). The deduced value (4,000 per hour for each "*Y*-element") is in good agreement with the observed one (3,600 per hour).

KONDO I., MURAYAMA T., MORI S., OKUDA H., SAKAKIBARA S., MAKINO T. and HONZAWA T. (Physical Institute, Nagoya University) **On the Observation of High Energy Cosmic Ray Particles by Cosmic-Ray Telescope No. 3. (II) Zenith Angle Dependence**——Using the newly built cosmic-ray telescope, directional intensity of high energy cosmic-ray particles (mu-mesons > 10 GeV, electrons > 150 MeV) was measured. In the course of measurement of zenith angle dependence, two sources of background pulses were noticed. *I.e.*, (1) pulses due to Čerenkov radiation in photomultiplier windows emitted by local shower particles. (2) Accidental coincidence pulses by noise of photomultipliers. (1) is much more important (~1/min, for a *Y*-element) and will be reduced by anticoincidence method while (2) has smaller effect (~0.1/min., N=2.10⁴/sec, τ=1.5. 10^{-7} sec). The counting rate of the telescope was corrected for these background effects and the zenith angle dependence of the intensity was obtained. This was in good agreement with theoretically estimated zenith angle dependence of high energy cosmic-ray intensity. From this zenith angle dependence, it was found that 50 percent of primary cosmic-ray particles which produce these high energy cosmic-ray particles have energies between 30 and 80 GeV for z=0° and 170 and 330 GeV for z=80°. The east west asymmetry of cosmic-ray intensity was found to be less than 3 percent for the energy range observed by this telescope, even at large zenith angle. Some preliminary results of continuous observation of cosmic-ray intensity by this telescope was also presented.

KAMIYA Y., SAGISAKA S., UENO H. and KATO S. (Nagoya University) **On the Construction of Cosmic-Ray Telescope with a Solid Iron Magnet**——In order to determine the sign of charge and the momentum in high energy cosmic-ray particle, a new cosmic-ray telescope with a solid iron magnet (Cosmic-Ray Telescope No. 4) is now under construction at Nagoya University. The design of this apparatus were reported in the preceeding paper presented the annual meeting, May 16-18, 1960 (published in J.G.G. Vol. XII, No. 1). This is preliminary report. The total magnetic flux in this magnet was measured by means of search coil and fluxmeter. The mean induction is 20 kilo gauss with excitation current 30 ampere and the variation of the excitation current is about ±1%. The efficiency of the neon hodoscope is about 80%.

KITAMURA T. (Geophysical Institute, Kyoto University) and KODAMA M. (Institutd of Physical and Chemical Research) **Time Variations of Cosmic Ray Intensity in the Antarctic Region (I) Atmospheric Temperature Effect and Diurnal Variation**——Cosmic-ray observations at Syowa Base,

Antarctica, have been carried out by using a Neher type ionization chamber during 1957-58 and a cubical telescope having two plastic scintillators since 1959, respectively. The amplitudes of diurnal variation of cosmic-ray meson component obtained from these observations are calculated in every month together with those at Mawson and Tokyo. It is seen from the figure (not given here) that the month-to-month variations of the amplitudes at the two stations in the Antarctic region are obviously different from that in the middle latitude station. This discrepancy seems to be due to the difference of the atmospheric temperature variations between the higher latitude and the middle. In order to extract the parts due to the atmospheric temperature effect only from the curves in Fig. 1, it was firstly corrected for the primary cosmic-ray variation by using the data of neutron monitor at Mawson. Then, the temperature coefficient of meson component was deduced from the several correlations between the different heights of isobar level and cosmic-ray intensities. In the results, the best correlation coefficient was obtained not in 300 mb, above which the best correlation in the middle latitude is usually found, but in 50 mb. Using the temperature coefficient thus obtained, 5%/km, it is possible to presume the amplitudes of diurnal variations of 50 mb isobar level, that is, they are about 12 meters in summer and about 7 meters in winter. To ascertain the above mentioned fact from the observational data of Radio Sonde, the diurnal variations of isobar levels at Tateno (Japan) and Kap Tobin (Greenland) are illustrated. There are no apparent seasonal changes in both 100 mb and 300 mb at the former station, whereas such a seasonal change is obvious at the latter corresponding to the same latitude as Syowa Base. Therefore, it is reasonable to say that the apparent seasonal change of diurnal variation on cosmic-rays at higher latitude are mainly due to the atmospheric temperature effect.

KITAMURA M. and TEZUKA T. (Meteorological Research Institute) **On the Daily Variation of the Cosmic-Ray Intensities (II)**——Data of cosmic-ray intensities observed by the neutron-monitors distributed all over the world during IGY are analysed to obtain the latitude dependence of diurnal and semi-diurnal variations of the cosmic-ray intensities for all days during IGY and storm times, respectively. The results are as follows: (1) The amplitude of the diurnal variation of cosmic-rays in the auroral zone for both all days and storm times are larger than those of other regions. Furthermore, increments of the amplitudes of the diurnal component are larger at high latitude than other latitudes. (2) The amplitude of the semi-diurnal variation shows the maximum value in the equatorial zone for both all days and storm times. And the energy dependence of increments of the amplitudes of the semi-diurnal variation during storm times are not so remarkable. (3) The maximum time of the diurnal variation for all days is about 11h at the equatorial zone and later in the high latitude. They are shifted towards the early morning in the low and middle latitude during storm times and are delayed in the auroral zone. (4) The maximum time of the semi-diurnal variation is about Oh at the equatorial zone and later in the high latitude. They are delayed in the high latitude during storm times.

KANNO T. (Department of Physics, Fukushima University) **On the World-Wide Distribution of the Daily Variation of the Cosmic Ray Neutron Intensity and its Variation (II).**——T_m, the local time of the maximum intensity in the diurnal variation of the cosmic-ray neutron intensity, was derived from the data of 39–43 stations during the period of I.G.Y. It seems that there are the latitude effect and the longitude effect in T_m. T_m in the vicinity of the geomagnetic equator advances and the magnitude of the latitude effect becomes large as the solar activity becomes intense. The longitude effect varies every month and the magnitude of its variation distributes with a certain tendency in the world. It may be suggested that the former is due to the modulation with magnetic clouds in the interplanetary space, and the latter is due to the deformation of the lines of force of the terrestrial magnetic field by the solar magnetic clouds.

OSHIO M. (Faculty of Science, Tokyo University) KODAMA M. (The Institute of Physical and Chemical Research) **World-Wide Distribution of the Cosmic-Ray Neutron Intensity and its Time Variation during Magnetic Storms**——In order to study physical state of magnetic cloud during magnetic storm, using the bi-hourly values of cosmic ray neutron intensities obtained at 35 stations during

IGY, intensity variations in the directions fixed to 12 local times are analyzed, where each station is divided into four groups according to the geomagnetic cut-off rigidity. At first, March 25, 1958 cosmic ray storm is adopted as an example not to be accompanied with large decrease in horizontal intensity of magnetic storm. Analysis seems to show that the amplitude of anisotropy of primary cosmic-ray particles reached the earth varies damping with 3~4 day period, and its direction becomes opposite in the latter half of the storm.

TORIZUKA K. (Tokyo Gakugei University) and WADA M. The Institute of Physical and Chemical Research, **Cosmic-Ray Storms in July 1959**——Cosmic-ray storms occurred on 15 and 17 July 1959 were studied. Those variations were recorded by means of a high sensitive meson detector installed at the Institute of Nuclear Study, Tokyo. The observation error was 0.1% of the mean intensity for the total count of several minutes. The same kind of observation was also carried out at Massatusetts Institute of Technology, U.S.A.. A comparison of the data of the two stations resulted the followings. (1) The variations of the 15 event at the two stations were in good parallelism, whereas those of the 17 event were in large difference with each other. (2) Two well separated increases were found during the decreasing period at 13–16 hr U.T., 15 July simultaneously at the both stations. The variations were: The first minimum was 1333 U.T., the first maximum was 1357, the second minimum was 1445, and the second maximum was 1506 in which the error of each time was 6 minutes. (3) The difference of the 17 event may be interpreted partly by the existence of many short lived increases during the period when the intensity was depressed. The increases were observed only at MIT which caused appreciable anisotropy of the intensity of coming particles.

KODAMA M. (The Institute of Physical and Chemical Research) **A Large Fluctuation of Cosmic Ray Intensity on July 18–19, 1959**——Cosmic ray intensity largely fluctuates during the recovering period 18th–19th of Forbush decrease on July 17, 1959. Cosmic ray stations represent such a fluctuation are not all over the world but limited to the geomagnetic latitude range 40°–70° and longitude range 20°–200°. This phenomenon occurs in not only the northern hemisphere but also the geomagnetic conjugate region in the southern hemisphere. It seems that Van Allen belt has a close relation with the present event.

TAKAHASHI H. (Faculty of Liberal Arts, Iwate University) **Latitude Effect of Cosmic-Ray Storms Associated with Magnetic Storms**——The statistical result about dependency of the latitude effect of cosmic-ray storms associated with magnetic storms on the magnetic storms is stated. The world-wide cosmic-ray data (14 stations) on mountain altitude and geomagnetic data obtained at Kakioka Magnetic Observatory during IGY are used. The result obtained is that the latitude effect of cosmic-ray storms associated with magnetic storms depends on the magnetic storms and it is greater on the large magnetic storm than on the small one. The further study will give the detailed discussions.

KUDO S. and MURAKAMI K. (Inst. Phys. Chem. Res.) **On the Relation between the Cosmic-Ray Diurnal Variation and the Other Phenomena**——It is very important to find out the substantial phenomenon related with the diurnal variation of the cosmic-ray intensity. In the present report, the frequency distributions of the amplitude of the diurnal variation, associated with the geomagnetic or solar events, were compared each other on the shape of the distribution. After the comparison of the distribution during a certain period, it is concluded that Type IV outburst in solar flare is a very essential phenomenon for the classification of the diurnal variation, rather than the cosmic ray storm or the other phenomena. And the change of the shape of the distribution was convinced with the lapse during one and half years. This change also is explainable, only if consider the change of the distribution of the diurnal variation associated with Type IV outburst.

TAKAHASHI H. (Faculty of Liberal Arts, Iwate University) **Correlation between Time Intervals from Onset of Cosmic-ray Storm to the Least Intensity and Solar Activity**——There is rather good correlativity between the yearly mean ($\bar{t}_I$) of time intervals from onset of cosmic-ray storm to the least intensity and the yearly mean ($\bar{R}$) of relative sunspot-numbers. $\bar{t}_I$ increase with increasing $\bar{R}$, and

they indicate a variation with solar cycle. This fact is interpreted by a simple solar cloud model.

KAMIYA Y. (Nagoya University) **Cosmic-Ray Storms and Type IV Solar Radio Outbursts**——In the preceeding paper (Rep. of Iono. and Space Res. in Japan, vol. XIII, No. 2, 1959), relations between the type of solar radio outburst, cosmic-ray storm and magnetic storm were studied using the data obtained during IGY, and the following results were obtained. (1) Almost all cosmic-ray storms were associated with Type IV solar radio outbursts. (2) The size of a cosmic-ray storm is independent of the meridian distance of the radio outburst, but that of a magnetic storm depends on it. In this paper, these results were more confirmed by using these data of the years 1959 and 1960.

SAKURAI K. (Geophysical Institute, Kyoto University) **Solar Protons and Electrons** ——We examine the behavior in the solar outer atmosphere and the geomagnetic dipole field of high energy protons and electrons which are produced from the sun: (a) we calculate, in detail, the motions of the solar cosmic-ray protons with a few Mev—several 100 Mev energies in the geomagnetic dipole field and then, seek for their precipitation lines on the earth's surface. In consequence, we obtain the following results; (1) there is anisotropy on their incidence, (2) their precipitation lines show the circular ones around the geomagnetic north pole, (3) their incident region is restricted in the polar cap region only, and (4) statistically, their incidence tends to concentrate to the morning hemisphere. Since the observed facts coincide well with the theoretical calculation, we may consider the features of the solar and the interplanetary magnetic fields in view of above results. (b) Next, we discuss the behavior, in the solar atmosphere, of the electron component of solar low energy cosmic rays. And then, we obtain some results that the energies of the electron component are order of 100Kev —1 Mev, and that these electrons will lose their energy by the synchrotron radiation in the sunspot magnetic fields (100 Gauss–1000 Gauss) extending in the solar outer atmosphere, and will not propagate into outer space. From this view point of these calculation, we are able to examine the acceleration mechanism and propagation one of the low energy cosmic rays produced from the sun.

SAKURAI K. (Geophysical Institute, Kyoto University) **The Trapped Orbits in the Störmer Theory**——We consider the trapping mechanism of charged particles in the earth's dipole magnetic field in view of Störmer theory. (1) As we can treat the motion of a charged particle in the axisymmetric magnetic field as a two dimensional problem, we are able to apply this method to the case of the dipole magnetic field and obtain the general forms of the equations of motion of a charged particle. (2) Since the forms of this problem are equivalent to the motion of a particle in a kind of potential field, we are able to examine the general properties of motion of this particle without solving the equations of motion. (3) In consequence, we obtain some results that there are two ways with regard to the trapping mechanism of charged particles as shown in the following; (a) periodic trapped orbits, (b) temporarily trapped orbits. It is possible to apply the above consideration to explain the cause of Van Allen radiation outer belt. Thus, we can examine the rigidities of the trapped particles in this belt and the stability of this trapping mechanism.

AONO Y. and KOIZUMI T. (Radio Research Laboratories, Japan) **Study on Stratification of *F* Region**——For the purpose of improving the $F1$ scaling practices, an investigation has been made on stratification of the F region of the ionosphere, using the daily f-plot focussed in 1958 for several stations in various latitudes so as to make clear the latitude effect. The stations, of which the f-plot is used in this study, are indicated in geomagnetic latitude as follows: (i) High latitude group Ottawa (N 56.9°), Moscow (N 50.8°), White Sands (N 41.2°), (ii) Middle latitude group Yamagawa (N 20.3°), Okinawa (N 15.5°), and (iii) Low latitude group Talara (N 6.6°), Chiclayo (N 5.3°). The results of this analysis give the conclusion describe below. The stratification of F region is so stable in high latitude in summer season, that the median and quartile values of the frequency at stratification seem meaningful, while they will be meaningless in every seasons or in any latitudes other than in high latitude in summer season because of the unstability of stratification. In general, the stratification becomes stable in every latitude, when $foF2$ at noon is less than 8 Mc. According to the investigation on the daily f-plot for various stations, most of the frequency at stratification appears in the value of (5 ± 1.5) Mc from 10h to 14h around noon. Therefore it might be

called the $F1$ layer for the stratification, at which the frequency changes in this frequency band. If the stratification appears sometimes in higher or lower frequency band, these stratification might be called F 1.5 or F 0.5 for example. The diurnal variation of the frequency at stratification is composed of such a repetition with period of about ten minutes that the frequency decreases in a sequential way and increases suddenly on appearance of a new stratification. Therefore, the geophysical investigation on the stratification of F region will be made only in use of the f-plot observed in every five minutes, at least on quarter-hourly basis. The monthly median value of the frequency at stratification will be affected by solar activity in a similar way as in fo$F2$ but not in a simple way of cosine value of the solar zenith angle as in fo$E$. In other words, it is noticeable that the monthly median value of fo$F1$ at a certain local day time has a semi-annual variation. The value of h'F does not change even if the stratification made rapid and sequential changes. The value of h'$F2$ makes in gradual and regular change of a large scale independing on the change of stratification of F region.

MATSUMOTO H. (Institute of Electronics, Kyoto University) **A Model of the Diurnal Variation of N (h) Profiles in the Ionosphere and its Conductivities**——A model of the diurnal variation of electron density profiles with height is constructed from the recent experimental data and the theoretical consideration for the purpose of the study of ionospheric physics. References are made to the following; (1) Above the height of F region maximum electron density (hm$F$)—Informations deduced from the measurement of Faraday rotation by O.K. Garriott. (2) Below the hm$F$—Tables of ionospheric electron density published by the Cavendish Laboratory. (3) Above the hm$E$ (E-F valley)-Results of rocket measurement in U.S. and U.S.S.R. (4) Below the hm$E$ a) A theoretical consideration checked by the results of impulse sounder and rocket measurements. We adopt a modified Chapman layer with the scale height with a linear increase vs. height i.e. $H=Ha+\Gamma(h-ha)$, and especially, the ion production rate used here in the case of glazing incidence is

$$I(\chi,h)=I_{mo}\exp(1+\Gamma)\{1-Z-g(\chi,h)\varepsilon^{-Z}\},$$

where

$$g(\chi,h)=\frac{a+h}{H}\sin\chi\int_0^{\chi}\left[\frac{H_a}{H}-\Gamma\frac{a+h}{H}\left\{\frac{a+h_a}{a+h}-\frac{\sin\chi}{\sin\lambda}\right\}\right]^{-\left(1+\frac{1}{\Gamma}\right)}\operatorname{cosec}^2\lambda d\lambda,$$

$$\chi=\frac{1}{\Gamma}\log\frac{H}{H_{mo}},\quad I_{mo}=I(o,\ h_{mo}),$$

$$H_{mo}=H_a+\Gamma(h_{mo}-h_a),$$

a: earth radius. We use a value of $\Gamma=0.2$ for the E region according to the recent results deduced by Kallmann from rocket and satellite measurements. b) A variation of the night time E region is based on the theoretical works by S. K. Mitra, and checked by the results of rocket measurements and those experimentaly obtained at Kyoto University. With this model, variations of electrical conductivities σ_0, σ_1, σ_2, σ_{xx}, σ_{xy}, σ_{yy} versus time and height are calculated for the ionosphere in the middle latitude.

HAKURA Y. (Hiraiso Radio Wave Observatory, Radio Research Laboratories), NAGAI M. and SANO K. (Kakioka Magnetic Observatory) **On the Relation between Magnetic Storm and Ionospheric Disturbances on Sept. 13th 1957**——An investigation was made on the relation between the world-wide patterns of ionospheric storms and corresponding current systems of geomagnetic storm for each stages of a severe upper atmospheric disturbance on Sept. 13th, 1957. A close relation of the polar magnetic disturbances to the occurrences of polar blackouts and storm Es was certified, suggesting that the current of polar magnetic storm flowed on the conductive region of disturbed lower ionosphere. It was also found that polar cap current system was produced several hours before the SC of geomagnetic storm, coinciding with the growth of polar cap blackout. After the SC, it developed its region to form the current system known as that of initial phase. At the main phase, ionospheric storm progressed to the world-wide scale; the regions of polar blackouts and storm Es elongated towards lower latitudes as the Dst field developed. And it was shown that auroral currents of bay-like disturbances at that stage, flowed exactly over such disturbed regions of high conductivity.

SINNO K. (Hiraiso Radio Wave Observatory, Radio Research Laboratories) **Some Characteristics on Solar Particles which Excite Abnormal Ionization in the Polar Upper Atmosphere**——A model on the ejection and propagation mechanisms which excite abnormal ionization in the polar upper atmosphere is presented from some statistical con-

siderations of the ionospheric data fmin. The evidence that the travelling time (Δt) between the major flares and the onset of polar absorptions show some heliographic relation, is reasonably interpreted by the present model; that is, the particles ejected from the flare are trapped into the magnetic cloud which would excite geomagnetic storm within 3 days, and are carried with rather slow velocity, then, the trapped particles could reach to the earth along the solar magnetic lines of force which extend to the earth, with high velocity. Existence of two different onsets of polar abnormal absorptions, sudden and gradual type of onset, are also favorable with this model.

NAGAI M., SANO Y. and YANAGIHARA K. (Kakioka Magnetic Observatory) **On the Dst and DS of Each Individual Magnetic Storm during IGY (I)**——For each individual storm, the averages of hourly mean value of 5 low latitude stations widely distributed in longitudes are used for *Dst* at equator. At a station *Dst* is considered to be $f(\theta)\cdot Dsto$, where *Dsto* is the *Dst* at equator and $f(\theta)$ is a function of the geomagnetic colatitude θ. For several high latitude stations, $DS=D-f(\theta)\cdot Dsto$ is calculated. *D's* are hourly values of the disturbance field during storm, and $f(\theta)$ is deduced from Chapman-Sugiura's statistical results. Then the ratio $\lambda=DS/SD_0$ is calculated for each hour of the first 2 days of the storm, where SD_0 is the mean disturbance daily variation by Chapman and Sugiura. Developments and decays of *Dsto* and λ are considered for each individual storm. In this first report, the analyses for 9 storms in the IGY and some preliminary consideration of the relation to the other phenomena, for example, activity of pt pulsation are described.

YAMAGUCHI Y. (Kakioka Magnetic Observatory) **S.i. Phenomena in the High Latitude**——In the previous paper, this author indicated the four foundamental types of s.i., based on the horizontal component traces. And the impulsive decreasing of the horizontal component occurred as frequently as the increasing impulse at Kakioka. In the case of ssc, the decreasing of the horizontal component is only rare in the middle or low latitude and mainly observed in the high latitude. The variations in the high latitude of the impulsive decreasing in the middle or/and low latitude are examined and resulted in that the decreasing components do not perfectly depend on the local time. The ssc are said to be expressed as follows;

$$\mathrm{Dst}+\mathrm{Ds}$$

and the decreasings of the horizontal component in the cases of reversed ssc are observed in the region where the horizontal components of Ds are negative. Thus, in spite of the resembrance of s.i. and ssc, the theory of ssc treating the sudden increase of the horizontal component does not seem to be suited in the original description. From the view point, some theories of ssc are reviewed.

YAMAMOTO M. and MAEDA H. (Geophysical Institute, Kyoto University) **The Simultaneity of Geomagnetic Sudden Impulses**——The start time of geomagnetic sudden impulses was examined by using IGY data. Analysis of rapid-run magnetograms at more than ten widely-separated magnetic stations yielded following results: (1) Time differences of sudden impulses around the earth were within one minute. (2) The sudden impulses always occurred first in high latitudes. (3) The average propagation velocity of sudden impulses between Honolulu and Koror was about 1300 km/sec. These results are very similar to those obtained by Williams for sudden commencements of magnetic storms.

YOSHIMATSU T. (Kakioka Magnetic Observatory) **Universal Time Daily Inequality of the Time of Maximum Depression of ssc in Storm-Time (II)**——In the previous paper (Memoirs of the Kakioka Magnetic Observatory, 1959) the author showed that the time interval between sc and the maximum depression of the horizontal intensity, T_L, undergoes a remarkable universal diurnal inequality against the beginning time of sc, expressed by the nearest hour in UT. From the point of view of this diurnal inequality it was also pointed out that some storms may be composed of two or more storms, and a few storms have abnormally shorter T_L's than would be expected, and so on. In this paper some other characteristics of T_L are further examined and reported as follows: (1) T_L does not show any diurnal inequality aganist both the times of the beginning of the main phase and the last phase. (2) The amplitude of the diurnal inequality of T_L is of comparable order to the mean of T_L, and the ratio of the maximum range of T_L to the mean value seems to become larger with decreasing geomagnetic latitude.

(3) The times of duration of the initial phase show the similar universal time diurnal inequality as that of T_L, though they are more scattered about the hourly mean values than those of the latter. (4) The universal diurnal inequality of T_L is closely connected to the distribution of the geomagnetic non-dipole field, especially in lower geomagnetic latitudes at the subsolar meridian corresponding to the universal time of sc.

MAEDA H. and ONDOH T. (Geophysical Institute, Kyoto University) **Evidence of the Ionospheric Propagation of Hydromagnetic Waves Caused by Nuclear Explosions over Johnston Island**——On examining carefully the induction magnetograms at Onagawa and Shimosato, Japan, we found geomagnetic changes which seemed to be due to high-altitude nuclear explosions over Johnston Island carried out on August 1 and 12, 1958. The changes started 10 sec later than the explosion time and lasted out about 30 sec. It seems from these results that the changes found at stations in Japan were due to hydromagnetic waves propagated in the upper ionospheric region across the lines of geomagnetic force from the explosion point. If so, the propagation velocity is estimated at about 500 km/sec for the first arrival and about 100 km/sec for the last arrival, on the average of both days. Moreover, if we assume that the initial changes at Honolulu were also caused by hydromagnetic waves, the average damping distance is estimated at about 1600 km.

MAEDA H., SAKURAI K. and YAMAMOTO M. (Geophysical Institute, Kyoto University) **Solar Radio Waves and the Earth Storms**——Recently, the studies on the relationships between the solar phenomena and the earth storms have been accumulated rapidly. Especially, it seems that the studies with regard to the relation of the solar radio emissions to the earth storms (cosmic ray storms, ionospheric storms and geomagnetic storms) will give a effective clue to the studies of the cause and the mechanism of these storms. We examine systematically this problem, with regard to various data during the periods of IGY and IGC, and, referring to the studies done already, try to explain the solar-terrestrial relationships either unificatively or quantitatively. At first, in Part (1), we investigate the following problems; (1) the relation of the geomagnetic storm producing solar flares and solar radio outbursts type II and IV, (2) the relationships among the geomagnetic storms, the associated cosmic ray increases, and the solar radio outbursts of type IV.

NAGATA T., OGUTI T. and THOMATSU T. (Geophysical Institute, University of Tokyo) **Polar Storms in July 1959**——Very close relation between geomagnetic variation and simultaneous luminosity of aurora was found in case of geomagnetic bay, giant pulsation, rapid pulsation and ssc* observed at Syowa station (lat. 69°.0S, long. 39°.6E). Horizontal disturbance vectors ξ of the geomagnetic field and zenith luminosity J of auroral green line, λ 5577Å, are mainly examined, with reference of maximum electron density n of sporadic E whenever possible. The results show that generally

$$J=K\,\xi^2.$$

In case of isolated geomagnetic bay, the amount of coefficient K is 3×10^{-3} KR/γ. In case of pulsations, however, periodic variations $\Delta\xi$ and ΔJ are superposed on respective back ground ξ_0 and J_0, and consequently

$$\Delta J=k\Delta\xi,$$

where k is in rough agreement with $2K\xi_0$. Relation between ΔJ and $\Delta\xi$ in case of ssc* is also in agreement with the above mentioned general conclusion. Therefore, this may give a direct evidence for that ssc*, or more generally polar part of ssc, is caused by impinging corpuscles in the E-region of the ionosphere accompanied by auroral displays. As for rapid pulsation of period less than 10 seconds, $\Delta\xi$ is under effect of impedance of electric conductivity owing to recombination of electrons and ions, expressed by

$$\dot{n}=Q-\alpha' n^2,$$

where Q and α' denote respectively ionization rate and effective recombination. Since $\alpha'\sim10^{-7}$ cgs in the auroral zone ionosphere, $Q\simeq\alpha' n^2$ holds for variations of period of longer than several minutes. But for variation of period of 10 sec or less, the impedance effect becomes significant. By considering this effect, $\Delta J/\Delta\xi\simeq7$ KR/γ for $\xi_0=200\gamma$ in case of rapid variation can be well explained in comparison with $\Delta J/\Delta\xi\simeq$ 1 KR/γ for the longer period variations. An exceptional case was found for geomagnetic giant pulsation, where $\Delta J/\Delta\xi\simeq7\times10^{-2}$ KR/γ for $\xi_0\simeq0$. This pulsation of period of about 6 min may be called the second type giant pulsation, and denoted by Pg II. In comparison with that geomagnetic bay, giant pulsa-

tion of type I, rapid pulsation and ssc* are originated in the *E*-region of the ionosphere accompanied by auroral displays of reasonable luminosity, Pg II is accompanied by very weak aurora. This result would indicate that Pg II is originated in outside of the ionosphere.

MAEDA R. (Faculty of Science, Tokyo University) and TAKEUCHI H. (The Institute of Physical and Chemical Research) **Temporal Variation and Spatial Distribution of Radiation at 1000 km above the Earth near Japan**——Temporal variation and spatial distribution at 1000 km above the earth near Japan are investigated by analyzing the data received at Itabasi, Tokyo from U.S. Satellite 1959 Iota during March and April in 1960. From April 6 th, to April 13 th great fluctuations of radiation occurred above the moderate latitude region, but were not seen above the low latitude. By cosmic ray decrease and geomagnetic storm on March 31 th, radiation intensity did not vary so much above the lower latitude as above the higher latitude. Spatial distribution of radiation at 1000 km above the moderate latitude is different from that above the higher latitude. The former has stationary contours of radiation intensity which are nearly parallel to the geomagnetic latitude lines, but the latter has irregularities and fluctuations. In order to interpret the variation and the distribution of the radiation, the outer zone and the slot of Van Allen Belt are worthy of consideration.

MATUURA N. (Geophysical Institute, Tokyo University) **On the Earth Storms (II) Interaction between the Solar Corpuscular Stream and the Earth's Magnetic Field**——The general features of electric current caused by charged particles trapped in the earth's magtic field have been examined. There are two parts in the electric current; one is caused by drift motions of trapped charged particles owing to the nonuniformity of the magnetic field and the other is caused by the particles of which guiding centres are lying outside the small volume under consideration and of which gyration paths are cutting the small volume. Therefore, the net electric current is given by the sum of the two. The latter part of electric current becomes complex when the physical quantities, such as density, magnetic field and particle velocity, vary sharply within the length of the order of Larmor radius of the particle. This problem has been discussed also. It is impossible to interpret the cause of main phase of the magnetic storm by a simple consideration of drift motion of the trapped charged particles. Further, the effect of temporal variation of magnetic field on trapped charged particles has been examined.

TOHMATSU T. (Geophysical Institute, Tokyo University) **On the Earth Storm (II) Energy and Flux of the Corpuscular Stream Impinging the Earth's Atmosphere (II)**——The simultaneous ionization and optical excitations by energetic electrons in the aurora are investigated by considering an isotropically incident electron flux whose energy spectrum is inversely proportional to the kinetic energy in the range between 100 eV and 100 KeV, as is consistent with the rocket results. The stationary electron density profile and the luminosities of N_2^+ negative bands and [OI] 5577 radiation are calculated by using available ionization and excitation cross sections. The results are compared with those from the optical and radio observations. It is concluded that the energetic electrons as well as the protons are able to be the main ionizing and exciting source in aurorae. The appearance of N_2 positive groups and its local time variation are discussed in view of the spatial and time variations of the energy spectrum of impinging stream. The intensity of the positive groups relative to the total luminosity becomes a usefull measure of the higher energy component of the incoming flux.

OGUTI T. (Geophysical Institute, Tokyo University) **On the Earth Storm (II) Interrelations among the Upper Atmosphere Disturbance Phenomena**——Statistical relations among the polar elementary magnetic storms including bay disturbances, giant pulsations, and short period pulsations, polar ionospheric disturbances, for example, abrupt increase in f_0Es and time change of h'Es, and time dependence of height of the auroral lower border, were examined. The occurrence frequency of positive, sharp negative and broad negative bays takes the maximum value centered around 18, 23 and 3h LT respectively, corresponding to the three maxima of f_0Es and of auroral appearance in high latitudes. Most of giant pulsations, however, occur in morning-daytime site (6–14 h LT) of the auroral zone, having no remarkable related disturbance in the ionospheric and auroral phenomena, and may therefore be attributable to the geomagnetic disturbances propagated

from the exosphere. Worldwide patterns of h'Es and auroral lower border are quite similar to each other. The former which takes the maximum height of about 140 km at 18-20 h LT in the auroral zone, gradually depressed through the night, and finally attains to the minimum hight of about 100 km at 3 h LT. It rises again at 6 h to about 120 km. From the facts mentioned above, it is concluded that the height of disturbances represented by anomalous ionization and simultaneous excitation in the lower ionosphere in the auroral zone is depressed systematically with respect to local time. The conclusion is supported also by the systematic increase of appearance probability of 1 P.G. in the auroral spectra thruogh the night. The local time dependence of the disturbance height may be due to the change in the sort and/or in the primary energy of impinging corpuscles during the polar earth storms.

KOKUBUN S. (Geophysical Institute, Tokyo University) **On the Earth Storm (II) Geomagnetic Disturbances in the Polar Regions (II)**——Characteristics of individual geomagnetic disturbances at the geomagnetic conjugate points in the northern and southern polar regions are examined based upon the IGY data. i) One to one correspondence of isolated bay-type variations between the geomagnetic conjugate points is especially good for case of local night time variations with typical auroral display. Correlation coefficient of horizontal disturbing force at Baker Lake (73.7°, 315.1°, geomagnetic coordinate) and Little America (74.0°, 312.0°, geomagnetic coordinate) amounts to 0.85. This result may indicate that the corpuscular stream originated in the exosphere tends to flow in along geomagnetic lines of force toward both their north and south ends in the ionospheric regions. In case of large magnetic storm, correlation of disturbing force between these two points becomes much poorer. This may suggest that relation between two points linked by a geomagnetic line of force is much disturbed owing to turbulent field in the outer atmosphere. It was found that giant pulsations of period $4^m \sim 15^m$ occurs simultaneously with nearly same period at the geomagnetic conjugate points in the local morning. It may be worthwhile to note further that bay-type variation in local night time has a tendency to shift westward to geomagnetic line of force. The velocity of this drift is $70° \sim 150°$/hr in order of magnitude.

KANEDA E. (Geophysical Institute, Tokyo University) **On the Earth Storms (II) Photometric Studies of Aurora All-Sky Camera Records**——As a new analytical method, ASCA-photoelectric analyser (ASCA-P.A.) has been designed for the quantitative analysis of aurora all-sky camera records. By the photometric method, ASCA-P.A. transforms aurora luminosity in a choiced area of movie-projected image of aurora all-sky records into deflection by pen writing oscillograph. Though the stage of analysis by ASCA-P.A. remains a preliminary one, future prospect of analysis by ASCA-P.A. is very promising.

YANAGIHARA K. (Kakioka Magnetic Observatory) **Observation of Geomagnetic Pulsations of Very Short Period, 0.1 to 10 sec**——Design of measuring apparatus of geomagnetic pulsations having very short period, 0.1 to 10sec, is outlined. Preliminary observations made at Kakioka by the apparatus, show some interesting results including the intermittent enhancements of activity during storms or bay-type disturbances. In particular, the pulsations of period, 2 to 4 sec, are predominant. On the other hand, irregular noises are observed at Kakioka with appreciable amplitudes in the geomagnetically calm period by the high sensitive apparatus. Stray currents of artificial origin, for example the electric railway near Tokyo, bring the noises, maybe. More accurate observation of pulsations by the apparatus will be made soon after at Memambetsu where artificial noises are reduced.

UTASHIRO S. (Hydrographic Division, Maritime Safety Agency) **On the Local Character of the Geomagnetic Pulsation Pc**——The author studied the results observed by induction magnetometers at the Japanese four stations (Memanbetsu, Onagawa, Simosato and Kanoya). From the results of the studies, local inequality of Pc was found. Period or mode of Pc change with latitude, and amplitude of Pc becomes larger with increasing latitude. Such local Pc type pulsation may be produced by the hydromagnetic oscillations in the region between the inner Van Allen Belt and ionosphere. Two mode of oscillations exist in this region, toroidal and poloidal oscillations. In the higher latitude the poloidal and toroidal oscillations are observed, in the lower latitude only the poloidal oscillation is observed. Therefore,

local Pc occurs frequently in the higher latitude than in the lower latitude. Then, the author studied on the local character of Pc observed at equator and lower latitude during the International Geophysical Year by rapid run magnetometer, that is, at the Koror, Guam, Apia and Honolulu Magnetic Observatory. Comparing the data of these observatories, Pc type pulsation occurs simultaneously at equator and lower latitude, and phase and period is the same at each observatory. From these phenomena, it seems that only Pc type pulsations produced by the poloidal part of the hydromagnetic oscillation are observed at equator and lower latitude.

KAWAMURA M., OUSHIMA H., KURUSU K. and YANAGIHARA K. (Kakioka Magnetic Observatory) **Wide Distribution of the Disturbance Vector of Pulsation Pc**——Disturbance vectors of pc having the period of about 20 sec are measured on the microfilms of the quick-run magnetograms for the 10 stations, *Lo*, *Mb*, *Kr*, *Gu*, *Ho*, *PB*, *Co*, *Si*, *Tu* and *Fr*. Worldwide development and decay of disturbance field for 24 hours of April 29 1958 are considered. Enhancement of amplitude in the day hemisphere is clearly noticed as deduced from the statistical daily variation of activity at one station. But the vector distribution changes so irregularly from time to time that it is very difficult to suppose an equivalent overhead current system.

SATO T. (1st Research & Development Center, Japan Defence Agency) **A Morphology of Geomagnetic Giant Pulsation**——Some statistical results of characteristics of geomagnetic giant pulsation that has period of about one to ten minutes are shown using the magnetograms during the IGY. Giant pulsation appears in the stations over the world, generally between 3^h and 2^h *L.T.*. The amplitude and occurrence frequency increase with increasing geomagnetic activity, especially, in great magnetic storm both are amplified. The results of the analysis of some great *SC* storms show that the giant pulsation is a world-widely simultaneous phenomenon, and at a certain universal time the periods and phases of the horizontal component are in coincidence with each other over the world. The results also show that the pulsation has a close relation with a bay disturbance in northern and southern hemispheres and the pulsation on the calm day in one hemisphere corresponds to the bay disturbance in other hemisphere. From these facts, the giant pulsation may be caused by the propagation of the hydromagnetic wave originated near the earth when the charged particles responsible for the bay disturbance impinge into the upper atmosphere. The micropulsation with a period of 10 to 40 seconds has also close correlation with a bay disturbance and the frequency of occurrence, amplitude dependency with latitude are similar with those of pulsation mentioned above. Therefore the origin of the former seems to be same as that of the latter.

KATO Y. (Geophysical Institute, Tohoku University) **Geomagnetic Pulsation Accompanying with the Solar Flare**——Usually we cannot detect the micropulsation caused by the solar flare in the record of the induction magnetograph, but at the time of very intense solar flares, experienced during IGY and also succeeded year, we observed very remarkable geomagnetic pulsations, continued in a few minutes having the period of 70–80 sec. There is a possibility that some kind of hydromagnetic oscillation in the earth's outer atmosphere will be excited by a sudden increase of solar radiation accompanying with the solar flare. If the intensity of external radiation, illuminating a highly conducting gas which rotates rigidly with the magnetic field, increases suddenly and the radiative equilibrium condition is established during a very short time in a rotating gas, then the torsional oscillation of line of force will be excited through the magnetic restoring force. Therefore it is probable to consider that above observed geomagnetic pulsation (especially it is very intense on the *E-W* component) is caused by these torsional oscillation of the outer atmosphere excited by the solar flare.

SAITO T. (Geophysical Institute, Tohoku University) **Geomagnetic Pulsations in the North American Region—Damped Type Pulsations Accompanying with ssc**——Using the rapid-run magnetograms in the North American region during IGY, fairly damped type pulsations accompanying with ssc are analyzed. These types of pulsations are divided into two groups as follows. (1) Pulsations with period of a few hundred seconds. At high latitude, ssc often accompanies with a damped type pulsation in the period range 200 to 300 sec. The amplitude of the pulsation increases with geomagnetic latitude and reaches its maximum at a little inside

of the auroral zone. (2) Pulsation in the period range 10 to 40 sec. Damping time of this type of pulsation is only a few minutes, nevertheless, it is very similar with *pc* type pulsation in the following characters. (i) Period contains is longer in the daytime than in the night time. (ii) Amplitude is larger in the daytime. (iii) Amplitude is also larger in the higher latitude. Then, a suggestion is given that the resonated hydromagnetic oscillation in the lower part of the exosphere gives rise to the above pulsation or *pc*, especially the former is excited by the hydromagnetic shock wave of ssc.

SINNO K. (Hiraiso Radio Wave Observatory, Radio Research Laboratories) **An Analysis on the Micropulsations from the Data of Wide Spread Observations**——Some results on the analysis of the micropulsations are presented from wide spread data of rapid run magnetograms during IGY. *Pc* micropulsation is divided into two frequency bands which is shorter than 30 seconds and longer than 40 seconds, shorter *Pc* and longer *Pc*, respectively. And, also, existence of another pulsation with 3 to 7 minutes period which is closely related with the longer *Pc*, is confirmed. *Pt* micropulsation can be divided into two groups: viz. Pt^- which is a *Pt* associated with a negative bay in the auroral zone and Pt^+ which is a *Pt* either associated with a positive bay or one which appears with no bay in the auroral zone. The equivalent current systems of the micropulsation *Pc*'s and *Pt*'s, are also derived. In this regard, a tentative discussion is given of hydromagnetic oscillations in the outer atmosphere are excited by solar corpuscular streams.

TAMAO T. (Geophysical Institute, Tohoku University) **Deviation of Geomagnetic Field and Hydromagnetic Characteristics in the Outer Exosphere**——With relation to hydromagnetic interactions between charged particles and the disturbing geomagnetic field, preliminary considerations on the mechanism of current system responsible to the deviation of geomagnetic field from the dipoler one which observed at 5~7 earth's radii by Sonnet et al. are given. In order to account this deviation, gas pressure of the order of 10^{-8} dyne/cm sec is required. Pressure expected only from thermal particles is not sufficient and the extention in space of deviation of field resulting from the consideration of pressure balance is too large to explain the observed results. Betatron acceleration of charged particles in the weak hydromagnetic disturbing region is discussed and the energy spectrum of particles characterized by the threshold velocity of the order of 10^8 cm/sec obtained. It may be likely that the source of the observed deviation of field is a ring current resulting from particles of few Kev diffused into and accelerated within the region of 7~12 earth's radii.

NAMIKAWA T. (Institute of Polytechnic, Osaka City University) **Propagation of Hydromagnetic Wave in the Earth's Upper Atmosphere**——The laws of reflection and refraction of hydromagnetic wave in the earth's upper atmosphere were found, using Piddington's equation of motion of partially ionized gases.

KAMIYAMA H. and OKUDA M. (Geophysical Institute, Tohoku University) **Intensity Variation of [OI] 6300A Emission in Night Airglow**——It has often been pointed out that the intensity of the red oxygen lines is closely related to the maximum electron density in the *F* region of the ionosphere. Introducing many parameters as well as maximum electron density, we carried out more reasonable calculation. Oxygen red lines in night airglow have been suggested to be produced through

$$\left.\begin{aligned} &O^+ + O_2 \xrightarrow{k} O + O_2^+ \\ &O_2^+ + e \xrightarrow{\alpha} O' + O'' \\ &O' \longrightarrow O + h\nu \end{aligned}\right\} \qquad (1)$$

the rate coefficient of which are denoted by k and α, respectively. Then, the intensity of red lines observed on the ground is given by

$$I = \alpha \int_{z_0}^{z_r} n[O_2^+] \cdot n[e] dz, \qquad (2)$$

where Z_0 is the lower boundary of the *F* region and Z_r is an appropriate altitude. As $n\ [O_2^+]$ can be approximated to $\frac{k}{\alpha} n[O_2]$, we can calculate the above equation. If we assume that the distributions of $n[O_2]$ and n [e] are given by

$$n[O_2] = n_a[O_2] \cdot \exp\{-\theta(Z - Z_d)\}, \qquad (3)$$

Z_d: datum level
$1/\theta$: scale height

and

$$n[e] = n_m[e]\left\{1 - \frac{(Z - Z_m)^2}{y_m^2}\right\}, \qquad (4)$$

y_m: semi-thickness of the layer
$(Z_0 = Z_m - y_m)$

we have

$$I=\frac{kn_a[O_2]n_m[e]}{\theta}\left\{\frac{2}{\theta y^2_m}\left(\frac{1}{\theta}-Z_m+Z_r\right)+\frac{(Z_m-Z_r)}{y^2_m}-l\right\}\cdot\exp\left\{-\theta(Z_r-Z_d)\right\}-\frac{2kn_a[O_2]n_m[e]}{\theta^2y^2_m}\left(\frac{1}{\theta}-y_m\right)\cdot\exp\left\{-\theta(Z_0-Z_d)\right\}. \quad (5)$$

when $Z_r=Z_m+y_m=Z_1$,

$$I=\frac{2kn_m[e]}{\theta^2y_m}\left\{n_0[O_2]+n_1[O_2]-\frac{1}{\theta y_m}\left(n_0[O_2]-n_1[O_2]\right)\right\}, \quad (6)$$

where n_0 and n_1 are the values at Z_0 and Z_1, respectively. Examining the observational data of the airglow and of the ionosphere, we found out the set of the highest correlation coefficients, being about 0.8 on the average, between them when we abopt the following values: $\frac{1}{\theta}=65$km and $Z_r=Z_1$ in winter, and $\frac{1}{\theta}=50$ km and $Z_r=300$ km in summer. We could also show that the observed results of the airglow intensity were given by $I_{obs}=I_0+I$, where I_0 is nearly constant in a course of a night. But I_0 exhibits the marked seasonal variation, and is suggested to be contributed from the lower part F region excluded from the parabolic ionosphere assumed by (4).

NAKAMURA T. (Tokyo Astronomical Observatory) **Latitude Effect of Oxygen Red Line of Night Airglow and their Relation to Ionospheric *F* Layer**——The photoelectric observations of the emission lines 5577A, 5893A, 6300A and *OH* bands in the infra-red in night airglow were made on board the m/s Soya in the 4 th JARE. The followings are the results reduced from the measurement of 6300A red-line. (1) The intensity of the red oxygen line shows remarkable increase in low latitude and also have high seasonal variation. (2) In low latitude, daily variation of the intensity is larger than in high latitude. It seems that this effect is due to the vertical motion of the emission layer in low latitude. (3) The absolute intensity R of the red line shows good correlation with Q which is expressed by

$$Q=K\int_{z_1}^{z_2} n(e)\cdot n(O_2)dz$$

where $n(e)$ is the electron density in the F_2 layer, $n(O_2)$ is the density of oxygen molecules, and K is the recombination factor of O_2 and O^+. From this fact we may conclude that the following reaction predominate in emitting 6300A line.

$$O^+ + O_2 \longrightarrow O_2^+ + O$$
$$O_2^+ + e \longrightarrow O^* + O^{**}$$
$$O^*(D) \longrightarrow O(^3P_2) + h\nu(6300)$$

The value of K becomes to about $1.3\cdot10^{-11}$ cm^3/sec in the F layer.

NAKAMURA M. (Institute for Optical Research, Tokyo University of Education) **Measurements of Altitude of the Glowing Layer of *OH* Infrared Bands in the Night Sky (I) Trigonometrical Method**——The glowing layers in the night sky are, in general, neither homogeneous nor stationary, but display strong variation spacially and with time. If any patches are observed simultaneously at two stations situated at an appropriate distance, one can find the altitude of the glowing layer by means of a trigonometrical method. The *OH* emission in the night airglow was observed at Kakioka, Ibaragi Prefecture and Maruyama, Chiba Prefecture, which situate about 135 km apart in almost north and south. Simultaneous observations were succeeded in three nights up to date. (Dec. 27/28, 28/29, and 29/30, 1959). Isophoto maps on which the intensity distribution of *OH* emission was shown by contour lines were drawn for each 30 minutes, and about 30 pairs of simultaneous isophoto maps were obtained. The altitudes are estimated at 74 km from the most probable shift of the simultaneous maps, 72 km from the intensity on the same meridians, and higher than 50 km and lower than 100 km from the time variations of the mean intensities of superposed area.

ONAKA R., NAKAMURA M. and TAKEZAWA S. (Institute for Optical Research, Tokyo University of Education) **Measurements of Altitude of the Glowing Layer of *OH* Infrared Bands in the Night Sky (II) Estimation by Van Rhijn Formula with Data taken at a High Altitude by Jet Plane**——To reduce the atmospheric extinction of light from the night airglow, measurements were carried out on a jet plane at a high altitude (elevation was about 13 km). Seven zenith distances—0°, 50°, 65°, 70°, 75°, 80° and 85° were surveyed. Six flights were carried out and measurements were performed about 15 times for each flight. The altitude of the glowing layer of *OH* bands was estimated by comparison with Van Rhijn formula at 60 km from the earth surface.

WAKAI N. (Radio Research Laboratories)

The Movement of *Es* Cloud and Night *E* Layer at Syowa Base——The movement of *Es* cloud; Using the sequences of ionograms at Syowa Base, the drift velocity of *Es* cloud was deduced from the change of the apparent height of oblique *Es* trace when it was assumed that *Es* cloud was moving horizontally toward or away from the station. Observed curves of apparent height versus time are classified roughly into two groups of different velocity of the motion. First group has a horizontal velocity of about 100 meters per second which is identical with the value obtained from the other method to measure the wind velocity in *E* region. On the other hand, second group has a velocity of 800 meters per second. It is noticed that the amount of the velocity is similar with the change of the position to be bombarded by ionizing agent. Night *E* layer; Several characteristics of night *E* layer were analyzed and com pared with those at other high latitude stations. Night *E* layer could be often observed prior to an increase of *Es* ionization and more frequently observed at night time even in winter when sun is below horizon at noon.

NAKAMURA J. (College of General Education and Tokyo Astronomical Observatory, University of Tokyo) **Spectra of Aurorae (I) Time and Space Statistics**——Aurorae may be classified into three types; (a) yellow-greenish one, (b) red lower border and (c) red upper border or red all over. Representative spectral lines of them are as follows; (a) *OIλ* 5577 line and N_2 N.G., (b) lst P.G. and *Hα* and (c) *OIλλ* 6300, 6363 lines. Space statistics were performed as to aurorae which were appeared at Showa Base (69°00S, 39°35'E) during 1959. Auroral maximal zone lies in (a) southern region of our base, (b) northern region of there and (c) somewhat southern bearings of there respectively. Their height may be as follows; (a) about 100 km, (b) 80～90 km and (c) abut 200～300 km. Time statistics: (a) type aurora appears at daily night time and has nearly constant local time sequences. (b) occurs with magnetic bay which maximum activity occurs near midnight. Always *Hα* line appears first and one hour or two later lst P.G. appears. (c) occurs accompanied by magnetic storms and it seems to have no correlation with local time.

NAKAMURA J. (College of General Education and Tokyo Astronomical Observatory, University of Tokyo) **Spectra of Aurorae (II) Doppler Shift of *Hα* Line**——Dispersion of auroral spectra taken at Showa Base was 320A per mm and it could be read to about 1.5A by Hartmann's formula. All of *Hα* and *Hβ* lines were suffered Doppler shift, and quantity of them varied by each direction along magnetic meridian. If we assumed the incident direction is coinside with the direction of magnetic lines of force (azimuth 350°, zenith angle 26°), above variation is well elucidated. The approaching velocity along lines of force distributes between $1.0 \sim 9.5 \times 10^7$ cm per sec, which maximum lies about at 3.0×10^7 cm per sec. A velocity component perpendicular to approaching one is about one third of the approaching velocity that is distributed between $0.5 \sim 3.0 \times 10^7$ cm per sec.

ONDOH T., KITAMURA T. and MAEDA H. (Geophysical Institute, Kyoto University) **The Relation of the Dawn Chorus to the Ionospheric Absorption of Cosmic Noise and the Auroral and Geomagnetic Activities**——We have studied the relation of the dawn chorus to the ionospheric absorption and the auroral and geomagnetic activities on geomagnetically quiet and disturbed days from September, 1959 to March, 1960, by using the data observed at College, Alaska. There is a negative correlation between the auroral activity and the chorus. This fact seems to imply a possibility that the chorus is absorbed by unusual ionization due to auroral particles. On the other hand, the correlation between the chorus and the cosmic noise is positive. This may mean that both the chorus and the cosmic noise are influenced by ionospheric absorption in a similar manner. If the origin of the chorus and the cosmic noise is independent of magnetic storms, there may be expected a functional relation between them. The origin of the chorus seems, however, to be affected by magnetic storms, so that the deviations from such a relation may be regarded as an effect of magnetic storms. These deviations are in a negative correlation to the magnetic K-index. This fact may imply that the exospheric region where the geomagnetic line of force starting from the earth's surface at 64° in geomagnetic latitude goes up on magnetically quiet days becomes inactive in generation of the dawn chorus with the increase of magnetic activity. Such a explanation will be clarified by using more data at other stations.

ONDOH T. (Geophysical Institute, Kyoto University) **On the Origin of the V.L.F. Noise in the Earth's Exosphere**——The radiation power of the Cerenkov radiation and the proton cyclotron radiation are respectively 1.7 $\times 10^{-24}$ watts. m^{-3} and 7.2×10^{-28} watts. m^{-3} at 2 earth-radii from the center of the earth on the geomagnetic line of force passing through the earth's surface at the geomagnetic latitude 60°, where the electron density is $5 \times 10^3/cm^3$ and the velocity of the protons is 10^9 cm/sec. As Ellis has pointed out, the Cerenkov radiation due to charged particles moving along the geomagnetic line of force gives the same type frequency characteristics as that of the travelling wave tube type amplification given by Gallet. The condition of the generation of the Cerenkov radiation and the operation of the travelling wave tube type amplification is given by $V_1 \cos\theta = \frac{c}{n}$ and $V_2 \approx \frac{c}{n}$ respectively, where V_1 and V_2 are the velocities of protons. When θ is small but not zero, we may consider that the whistler mode radio waves radiated by the mechanism of the Cerenkov radiation are amplified by the amplification mechanism of the travelling wave tube type due to different charged particles at the different part in the space and the time. At 2 earth-radii from the center of the earth on the geomagnetic line of force starting from the earth's surface at the geomagnetic latitude 60°, we have for the total emission in a column of length 200 km which consists of fast protons (density $10^{-1}/cm^3$), 1.4×10^{-22} watts. m^{-2} $(c/s)^{-1}$. The received power flux of dawn chorus signals is of the order of 10^{-16} to 10^{-14} watts. m^{-2} $(c/s)^{-1}$. Thus we can not obtain theoretically the received power flux without the gain of amplification greater than 60 *db*.

INOUE Y. and HASHIZUME S. (Group of Radio-physics, Electrical Engineering Division, Meguro Research Laboratories, National Defence Agency) **Exospheric Radio Sounding**——Two new methods studying the exosphere are presented. (1) Whistler Compression Filter (WCF); A whistler is generated by a lightning impulse. Its dispersion is formed in the course of propagating along the dispersive delaying path in the exosphere. Its delaying time is $t_d = \frac{D(\theta_m)}{\sqrt{f}}$ for short whistler, where $D(\theta_m)$ is the dispersion at the magnetic latitude θ_m. After a whistler receiver, a phase equalizer with the frequency response of $\exp\{2\pi i(2D(\theta)/\sqrt{f})f\}$ is followed: This equalizer compensates the dispersive delaying time of a whistler and converts it into a sharp pulse like an original lightning inpulse. WCF does not enhance noises and disperses sferics. It has a high discrimination for a whistler. By WCF, the 24 hr clock-run observation becomes possible. (2) Inverse Long Whistler (ILW); A signal is transmitted with the inverse frequency dispersion to a long whistler. The signal is converted into a sharp pulse by the dispersive delay in the course of propagation in the exosphere. The signal equivalent to a lightning impulse in the greatest class is as follows:

transmitting power.....3KW
transmitting duration.....1 sec
frequency dispersion range 1–10KC

The echo-pulse can be detected with an ample S/N. Furthermore, by adjusting the frequency dispersion of the signal, we can know precisely the characters of the propagation of VLF-radio waves in the exosphere. ILW can be transmitted in sferics-calm times. By ILW, it is possible to study the propagation exactly along the geomagnetic line of force. As its PRF is some 0.25 c/s in middle latitudes, one can investigate the rapid variations of the exospheric characteristics.

昭和36年3月1日　印刷
昭和36年3月5日　發行
第12卷　第2號

編輯兼發行者　日本地球電氣磁氣學會
代表者　長谷川万吉

印刷者　京都市南區上鳥羽唐戸町63
田中幾治郎

賣捌所　丸善株式会社京都支店
丸善株式會社 東京・大阪・名古屋・仙台・福岡

JOURNAL OF GEOMAGNETISM AND GEOELECTRICITY

Vol. XII No. 2

1961

CONTENTS